Graphene Oxide Microelectrodes for Detection of Hydrogen Peroxide

By

Anuranga Iranji Bandara Udadeni Pathirannehelage

Submitted to the graduate degree program in the Department of Chemistry and the Graduate Faculty of the University of Kansas in partial fulfillment of the requirements for the degree of Master of Science

---

Chairperson, Michael A. Johnson , Ph. D.

Susan M. Lunte, Ph. D.

Richard S. Givens, ph. D.

Date Defended: January 26, 2017

The thesis Committee for Anuranga Iranji Bandara Udadeni Pathirannehelage certifies that this is the approved version of the following thesis

Graphene Oxide Microelectrodes for Detection of Hydrogen Peroxide

---

Chairperson, Michael A. Johnson , ph. D.

Date Approved: January 31, 2017

Abstract

Hydrogen peroxide is a membrane-permeable reactive oxygen species (ROS) and a neuromodulator. Here, we enhanced the electrochemical detection of hydrogen peroxide by modifying a carbon-fiber microelectrode by dip-coating in slurry consisting of graphene, a conductive material with a honeycomb structure, and electrochemically depositing Nafion, a fluoropolymer. Morphological characterization of the modified electrode by scanning electron microscopy (SEM) revealed a fine coating of Nafion/graphene at the electrode surface and elemental mapping by energy dispersive X-ray spectroscopy indicated the presence of oxide groups, characteristic of graphene. Flow injection analysis of hydrogen peroxide using this modified electrode revealed a 5.3-fold increase in the oxidation signal compared the unmodified electrode. Moreover, the electrode kinetics were similar to those observed with bare carbon-fiber microelectrodes. These results suggest that this electrode may be useful for detection of transient hydrogen peroxide concentrations in biological systems.

Post-chemotherapy cognitive impairment (PCCI), also known as ‘chemo brain’, is a decline in cognitive function experienced by patients who have undergone chemotherapy treatment. Recent studies have shown that up to 30% - 70% of patients who receive chemotherapy treatment suffer from a general decline in complex problem solving, memory, learning, and motor function. Previous studies in our group have revealed that dopamine release and uptake, evoked in the striatum by electrical stimulation and measured with fast-scan cyclic voltammetry at carbon-fiber microelectrodes (FSCV), are impaired as a result of chemotherapy treatment. Although the reasons underlying this decrease in release are not clear, it is possible that terminals may be damaged by ROS. Hydrogen peroxide is an important ROS that has the potential to not only cause cellular damage, but also is a participant in the regulation of dopamine (DA) release. It is also known to be an inter- and intra-cellular signaling molecule. In the striatum H_2O_2 is generated from glutamatergic AMPA receptor activation in

medium spiny neurons. H_2O_2 can inhibit DA neuron firing via activation of ATP sensitive K+ (KATP) channels. Furthermore an imbalance of H_2O_2 generation and metabolism can cause neurodegeneration. To investigate the role of hydrogen peroxide in chemo brain, we measured sub-second changes in hydrogen peroxide levels with FSCV in striatal brain slices from rats receiving chemotherapy and Saline treated rats. We utilized two common chemotherapeutic agents, Carboplatin and 5-fluorouracil (5FU). We found that, upon treatment of slices with mercaptosuccinate, an inhibitor of glutathione peroxidase, the frequency of occurrence and the magnitude of transient increases in hydrogen peroxide levels were greater in carboplatin-treated rats compared to Saline control rats.

Affectionately dedicated to my ever loving parents, and my family

especially my loving husband and sons,

Akain and Vidun

Acknowledgement

I would like to express my utmost thanks and appreciation to my research advisor Prof. Michael Johnson for his support throughout my graduate life. I really appreciate the opportunity that you gave me to start my graduate research in your laboratory in the summer of 2014. As my research mentor, I thank you for your guidance and encouragement. I really appreciate your continuous support, kindness and helpfulness that you have given in my entire graduate career, especially that you were supportive during my hard times. I believe that it has been an honor and a privilege to work for you. I would also like to take this opportunity to thank Prof. Craig Lunte for his support and encouragement for me to get into the graduate program in the Department of Chemistry at the University of Kansas. Moreover, I would like to express my deepest gratitude to Prof. Richard S. Givens for allowing me to perform research in his laboratory as a volunteer in the summer of year 2013. I would also like to thank the group members in the Johnson's group including the former members and all the collaborators in the University of Kansas. Also thanks go out to my committee members, Prof. Susan M. Lunte and Prof. Richard S. Givens. I would also take this opportunity to thank the University of Kansas for the support given. Also I would like to thank Dr Thapa Chetri premsingh, Scanning electron microscopy Lab,University of Kansas for help with electrode surface analysis and Racheal Ginther for help with Chemotherapy treatments and for anesthetizing and decapitating animals.

My heartfelt and sincere thanks go to my husband, Dr. Sanjeewa N. Senadheera, for his patience and for his supportive encouragements to finish my graduate studies. Also I should specially thank my elder son Thenuja Akain Senadheera for understanding and supporting me throughout my graduate life and also to Vidun Nimnath Senadheera for providing love, joy, and cheer.

I would like to express my deepest gratitude to my loving parents for taking care of my kids while I was struggling with my studies and research and also for their endless support and

encouragement throughout my academic carrier. It would be impossible to achieve my goals without your support. Finally, I would like to thank all of my extended family and friends for their encouragement and support.

Table of Contents

Chapter 3

List of Abbreviations

aCSF	Artificial cerebrospinal fluid
ALDH	Aldehyde dehydrogenase
AMPA	α-Amino-3-hydroxy-5-methyl-4-isoxazolepropionic acid
ADP	Adenosine diphosphate
ANOVA	Analysis of variance
ATP	Adenosine triphosphate
BBB	Blood-brain barrier
°C	Centigrade (celsius)
CCD	Charge-coupled device
CNS	Central nervous system
CNTs	Carbon nanotubes
CV	Cyclic voltammogram
CFMEs	Carbon fiber microelectrodes
cps	Characters per second
DA	Dopamine

DNA	Deoxyribose nucleotide
DOPAC	3,4-Dihydroxyphenylacetic acid
DOPAL	3,4-Dihydroxyphenyl-3-acetaldehyde
DPN	Diabetic peripheral neuropathy
DNA	Deoxyribonucleic acid
e	Electron
E	A potential
EDX	Energy dispersive X-ray spectroscopy
eV	Electronvolt
F	Faradays constant
FSCV	Fast-scan cyclic voltammetry
5-FU	5-Fluorouracil
GHS	Glutathione peroxidase
GO	Graphene oxide
H_2O_2	Hydrogen peroxide
HEPES	4-(2-hydroxyethyl)-1-piperazineethanesulfonic acid
Hsp 90	Heat shock protein 90
5-HT	5-Hydroxytryptamine
IR drop	The potential drop between the working electrode and the reference electrode
Kg	Killogram

KU-32	N-{7-[(2R,3R,4S,5R)-3,4-dihydroxy-5-methoxy-6,6-dimethyl-tet-rahydro-2H-pyran-2-yloxy]-8-methyl-2-oxo-2H-chromen-3-yl}acetamide
LOD	Limit of detection
LOQ	Limit of quantification
M	Molarity
18.2 MΩ	Milli-Q water
MCS	Mercaptosuccinic acid
mg	Milligram
ms	Milliseconds
mM	Millimolar
MSNs	Medium spiny neurons
MAO	Monoamine oxidase
µm	Micrometer
MWNT	Multiwalled carbon nanotubes
n	Number of electrons
N	Number of molecules
nA	Nanoamphere
NADPH	Nnicotinamide adenine dinnucleotide phosphate (reduced form)
Nox	NADPH Oxidase
nM	Nanomolar

ns	Nanoseonds
O_2	molecular Oxygen
PCCI	Post chemotherapy cognitive impairment
PEDOT	Poly(3,4-ethylenedioxythiophene)
Q	Integral of the current
QoL	Quality of life
RF1	Redoxfluor-1
rGO	Reduced graphene oxide
RNA	Ribonucleic acid
ROS	Reactive oxygen species
s	Seconds
SEM	Scanning electrom microscopy
SN	Substantianigra
S/N	Signal to noise ratio
SOD	Superoxide dismutase
SUR	Sulfonylurea receptor
$t_{½}$	Half-life
TS	Thymidylate synthase
TES	*N*-tris(hydroxymethyl)methyl-2-aminomethanesulfonic acid
V	Volt

XPS	X-ray photoelectron spectroscopy
*	Significant

CHAPTER 1

Introduction

1.1 Importance of detecting neurotransmitters and neuromodulators in the brain

The human brain contains approximately 100 billion neurons that communicate by transmission of electrical and chemical signals[1]. Although specific structural configurations vary, neurons signal other neurons and cells by release of chemicals through projections called axons and receive chemical signals through dendrites, which also project from the cell bodies (soma). The gap between an axon terminal of the presynaptic neuron and the dendrites of the post synaptic neuron is called a synapse and chemical communication across synapses is called synaptic transmission. When a chemical signal is received, neuronal cells are activated and an action potential is generated. This action potential propagates along the axon to the axon terminal where small vesicles filled with neurotransmitters are located. These vesicles are stimulated by the action potential and the neurotransmitters are released to the extracellular space[1].This whole process is called exocytosis. The released neurotransmitters bind to the neurotransmitter receptors on the surface of another neuron, passing the chemical message. Hence, neurotransmitters are essential for neuronal communication.[2]

Neurotransmitters are chemicals that promote communication among the brain's billions of nerve cells. Dopamine, for example, plays significant roles in many physiological or neurodegenerative conditions, including Parkinson's disease,[3] Huntington's disease,[4] and multiple sclerosis.[5] Often, in these and other conditions, neurotransmitter release, especially that of dopamine, are impaired. Hence, it is essential to study the chemical dynamics of neuroactive molecules to understand the mechanisms underlying the neurodegenerative disease states. Another neurochemical, hydrogen peroxide, is a reactive oxygen species (ROS)

[6, 7] that has also been implicated as neuromodulator[6] and has been shown to exhibit control over dopamine release at presynaptic terminals.

Neurotransmitter and neuromodulator levels may be quite low. For example, basal concentrations of DA in the striatum are around 10-30 nM.[8-10] Therefore, sensitive analytical methods, capable of measuring rapidly changing concentrations of these chemicals, are needed for their analysis in order to resolve details of neuronal function. Electrochemical methods, such as amperometry, various potential pulse methods, and cyclic voltammetry that may be well suited for this purpose, have been applied to monitoring neurotransmitter fluctuations in living tissues[11-14]. In these methods the oxidation or the reduction of the neurotransmitters are detected at an electrode. Of these methods, background-subtracted, fast-scan, cyclic-voltammetry at carbon-fiber microelectrodes (FSCV) have proven useful because it affords researchers with micron-scale spatial resolution, millisecond temporal resolution, and good chemical selectivity.[15]

In this work, we used FSCV to measure hydrogen peroxide (H_2O_2), an important membrane permeable reactive oxygen species (ROS) and a neuromodulator that has been shown to function in inter- and intra-cellular signaling. As an example, H_2O_2 modulates locally evoked dopamine release in terminals of the brain striatum by interaction with ATP sensitive K+ channels located on presynaptic dopamine terminals[6]. The remainder of this chapter focuses on methods used to electrochemically measure molecules in the brain. Next, modifications to carbon-fiber microelectrodes aimed at enhanced limits of detection are briefly addressed. Finally, the importance of H_2O_2 and the application of FSCV for its measurement are mentioned.

1.2 Electrochemical methods commonly used in neurotransmitter measurements

1.2.1 Constant Potential Amperometry at Carbon-fiber microelectrodes

In constant potential amperometry, the electrode is held at a steady potential (holding potential), and any electroactive molecule at the electrode surface will be oxidized or reduced, thereby producing a faradaic current, which is plotted against time. From those current vs. time plots, the total number of electrons transferred can be determined by integration of the current (Q) over the time period at which the peak was registered. In accordance with Faraday's Law (see below), the total number of electrons is directly proportional to the number of molecules (N) electrolyzed at the electrode surface.[16, 17]

$$Q = nNF$$

Faraday's Law (1)

Where, F is the faradays constant (96,485 $Cmol^{-1}$), n is the number of electrons transferred.

Because constant potential amperometry avoids complications associated with scanning the potential, temporal resolutions of one ms are routinely used when combining this technique with carbon-fiber microelectrodes. This outstanding temporal resolution allows real-time measurements that can resolve the time course of exocytosis release events. For example, constant potential amperometry has been used to determine that 30,000 molecules per vesicle are released from adrenal chromaffin cells.[13, 18] Nevertheless, the principle drawback of amperometry is lack of chemical selectivity; hence, it is not well suited for measurements containing complex mixtures of electroactive species, such as those present in the brain. Another approach capable of obtaining high-temporal resolution measurements, while at the same time providing additional chemical information of the chemical measured, is FSCV.

1.2.2. Fast-scan cyclic voltammetry at carbon-fiber microelectrodes (FSCV)

1.2.2.1 Introduction.

As stated previously, although amperometry has outstanding temporal resolution, it lacks chemical selectivity. Therefore, because the brain mixture of electroactive species is so complex,amperometry is not well-suited to selectively measure neurotransmitter/ neuromodulator release in this environment. For this purpose, we used fast-scan cyclic voltammetry (FSCV) at carbon-fiber microelectrodes. This technique provides sub-second temporal resolution and good chemical selectivity in that a cyclic voltammogram (CV), which serves as a signature for a given chemical species, is produced. However, before discussing the details of FSCV, we first discuss general aspects of voltammetry.

1.2.2.2 Voltammetry

Voltammetry became popular among scientist with the invention of the polarography in 1922 by Jaroslav Heyrovsky. In Voltammetry, analysis of the analyte involves measuring the current flow (i) while applying a potential (E) to the electrode surface. Potential is varied and the current is monitored over a time period. Analytes are oxidized or reduced at the electrode surface, and the resulting faradaic current response is measured. A primary advantage of voltammetry is that it provides excellent sensitivity and a large,useful linear range. In conventional voltammetry using macroelecrodes , a three electrode system (see Figure 1), consisting of a working, counter, and reference electrodes is typically used.

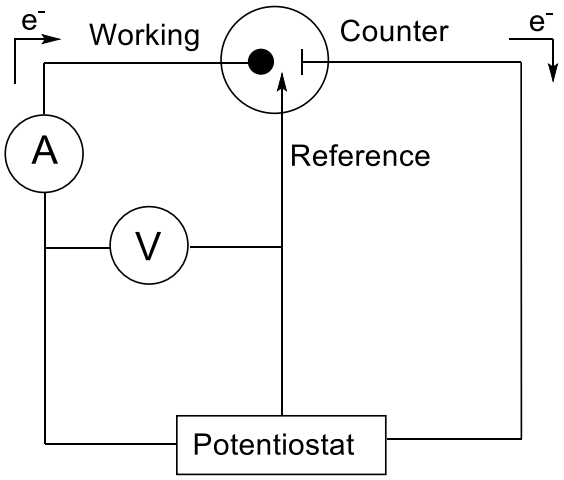

Figure 1. Schematic diagram of three electrode system

This arrangement has the advantage of eliminating IR drop, which is the decrease in potential applied to the cell that occurs due to the resistivity of the chemical environment (R). This phenomenon is dependent upon Ohm's law, E = IR, where E is applied potential (in V), I is current (in mA), and R is the resistance of the chemical environment. At high currents and resistances (MΩ), the amount of IR drop is sufficient to distort the current trace of a voltammogram because as applied potential becomes greater, the difference between applied potential and actual potential applied to the cell becomes greater.[19] As will be discussed below, despite the brain being a highly resistive environment, a two-electrode system can be used for FSCV since the magnitude of the currents measured is on the order of nA.

1.2.2.3 Cyclic voltammetry

Cyclic voltammetry is used in a variety of applications, including compound identification in general research, environmental, and neuroscience. This technique can provide useful information such as electrode properties, reaction kinetics and quantitative measurements of a

number of substances. In cyclic voltammetry, the applied potential is scanned to a different selected potential over a specified time interval and then scanned back. These cycles are repeated continuously as needed. When initially sweeping to a more positive potential, the analyte is oxidized. When scanning back to the original potential, if the reaction were reversible, the oxidation product will be reduced. The resulting current from the redox events during the cyclic sweeping is plotted against the applied potential to obtain a cyclic voltammogram (CV). The voltammogram of an analyte has a characteristic CV with a unique shape[19]. Hence, this method can be applied for the identification of a single species among several other substances without the requirement of further separation.

Cyclic voltammetry also allows determination of electrochemical reversibility by inspection of CVs. For a reversible electrochemical reaction, the criteria are as follows: (1) the difference in potential (E) at which the oxidation and the reduction peaks occur should be less than 0.058 V/n, where n is the number of electrons transferred in the redox reaction; (2) Oxidation and reduction current should be very close.[20] Electrochemically reversible reactions obey the Nernst equation.[16]

1.2.2.4 Fast Scan Cyclic Voltammetry at carbon-fiber microelectrodes

Fast Scan Cyclic Voltammetry (FSCV) is a variation of cyclic voltammetry and a powerful electroanalytical technique for measuring sub-second changes in neurotransmitter levels.[15] This electrochemical method was developed in 1980s by Jullian Miilar and colleagues in London.[21, 22] Compared to cyclic voltammetry, FSCV utilizes a much faster scan rate (up to 1×10^6 V/s). By applying a fast scan rate, voltammograms can be acquired rapidly within milliseconds.[23] FSCV provides good temporal resolution: 100 ms per CV as applied in our work. FSCV at carbon-fiber microelectrodes has been successfully used for the detection of neurotransmitters in biological systems. In FSCV, a triangular wave form is applied to the electrode at a high scan rate and the

electroactive species are oxidized and reduced at the electrode surface. The resulting faradaic current is measured.

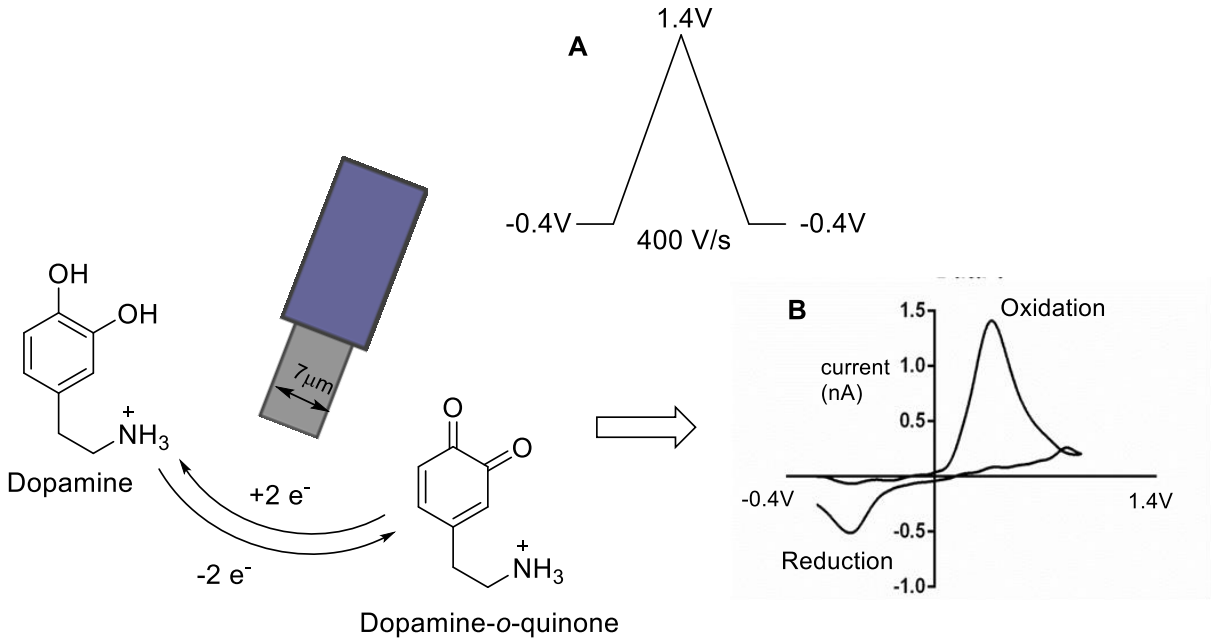

Figure 2. (A) Wave form applied, (B) Back ground subtracted cyclic voltammogram for DA. Holding potential at the electrode surface is insufficient to oxidize DA. Then the potential is linearly ramped to an oxidizing potential (1.3V) and back to -0.4V at a high scan rate (400V/s). DA is oxidized in the positive sweep in to dopamine-*o*-quinone and reduced back in to DA in the negative sweep. This process is shown in Figure 3. Electron flux is measured as current. Furthermore, resulting current is directly proportional to the number of molecules that undergo oxidation.

When applying fast scan rates, a large background current arises from the charging of the electrical double layer which is proportional to the capacitance of the electrode. To resolve this

problem, background current is subtracted. Figure 3 illustrates how the background subtraction is achieved.

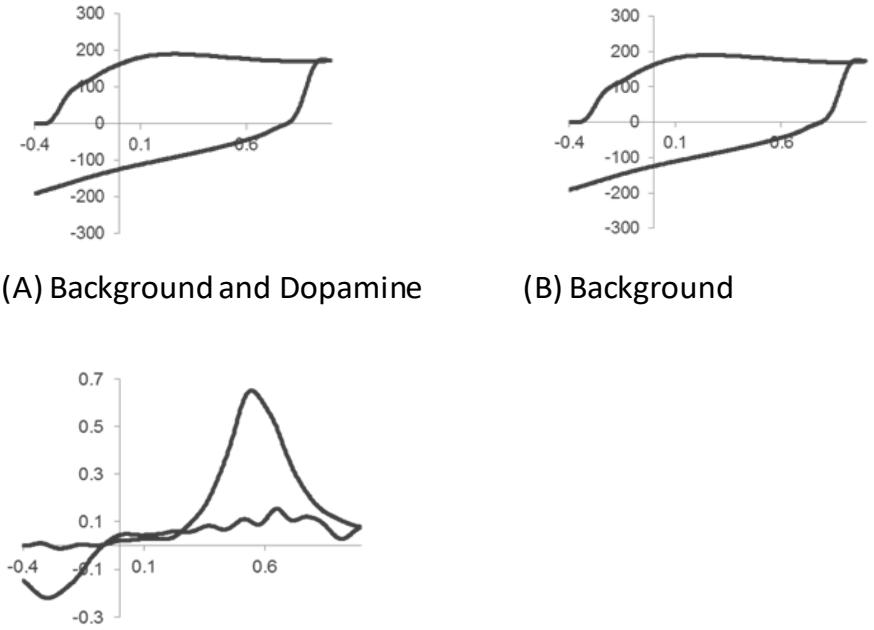

Figure 3. Back ground subtraction to obtain the cyclic voltamogramm. Substracting the back ground signal from the back ground and the dopamine signal

The resulting CV provides a chemical signature used to identify the species detected.[24, 25] Calibration factors obtained from standards of known concentrations are used to convert the peak currents in to concentrations. Due to the advantage of chemical selectivity, FSCV has been widely used *in vitro* and *in vivo* to detect a vast number of electroactive biological compounds such as dopamine, 5-HT, serotonin and norepinephrine.[26-28] Dopamine is the most common biogenic amine which is studied using FSCV; however, other electroactive species have been measured. These include serotonin,[29] norepinephrine, adenosine,[30] and hydrogen peroxide.[31]

Carbon fiber microelectrodes (CFMEs) were invented in late 1970s by Francois Gonon and colleagues[32, 33]. Most current biological research with electrochemical methods is done with carbon-fiber microelectrodes due to their many beneficial properties including biocompatibility, inert nature, low cost, high tensile strength and wide potential window[23, 34, 35]. These electrodes are fabricated using carbon fibers which are typically on the order of 5-10 μm in diameter, although larger and smaller diameters may be used. Generally speaking, fabrication in our laboratory is simple: single carbon fibers (7 μm in diameter) are aspirated into glass capillaries and pulled using a heated coil puller and trimmed with a scalpel to the desired length. The carbon-fiber is sealed by dipping in an epoxy resin. Excess resin is removed by dipping the electrodes several times in toluene and then cured by baking in an oven for 1 hour at 100 °C. An example is shown in Figure 3. The electrodes are back filled with 0.5 M potassium acetate in order to establish an electrical connection. Different geometries of microelectrodes include disk, elliptical, needle, double barrel and band electrodes, and each has it's own unique characteristics and may be used for different purposes.[23, 36]

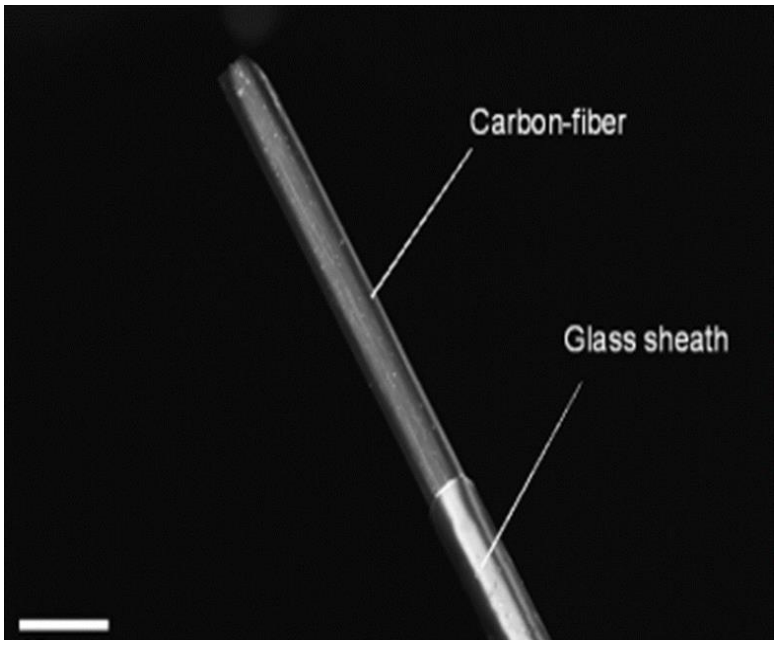

Figure 4. A scanning electron microscopy image of a carbon fiber microelectrode

As mentioned previously FSCV coupled with CFMEs is been used for years to distinguish and identify readily oxidizable biological compounds such as dopamine and serotonin. Specifically, this electroanalytical method is ideal for monitoring the chemical dynamics of neuroactive molecules and other electroactive molecules. Hence, this is an appealing analytical tool for detecting a wide range of species in the brain. Waveforms may be optimized for detection of different chemical species. For example dopamine, a catecholamine commonly detected using FSCV at CFME[28, 37], is often monitored by ramping the potential from -0.4 V to 1.3 V and then back to -0.4 V (Figure 4b).

In addition, non-electroactive species also can be detected using FSCV couple with modified CFMEs. Often CFMEs are coated with an enzyme to convert the non-electroactive species to an electroactive species.[38] Oxidase enzymes are commonly used for this process, especially for the detection of glutamate, glucose, lactate and choline. Here, H_2O_2 is generated

as the final product and can be electrochemically oxidized and detected on the electrode surface.[31, 39] For instance, glucose is converted to H_2O_2 by the enzyme glucose oxidase. Detection of H_2O_2 using FSCV coupled with CFMEs will be explained in more depth in Chapter 2.

1.3 Modified electrodes

In general, modified electrodes can be divided in to several categories, including those with derivatized surfaces, polymer coated electrodes, and functionalized electrodes.[40] Modified electrodes often take advantage of enhanced electron transfer kinetics. Moreover, modified electrode surfaces may provide several other benefits, including improved sensitivity due to increased surface area, improved selectivity toward the analyte of interest due to the presence of immobilized functional groups and dopants, and fast diffusion kinetics.[40, 41] Examples of materials used for electrode modifications include nanostructured materials and substances including nanoparticles, carbon nanotubes (CNTs), graphene and its derivatives, metals, alloys, inorganic substances and polymers[30, 40, 42-44]. After modification, it is critical to characterize the electrode surface to ensure proper modification. Techniques that have been used include Raman spectroscopy, scanning electron microscopy (SEM), and X-ray photoelectron spectroscopy (XPS).[45] Additionally, electrochemical characterization methods, including cyclic voltammetry[46] and FSCV,[31, 47] have been used. In this work, carbon-fiber microelectrodes are modified with graphene. These modifications are discussed in more detail in Chapter 2.

1.4 Overview.

The next two chapters discuss developing a graphene oxide/Nafion modified carbon-fiber microelectrode with enhanced sensitivity for H_2O_2 detection (Chapter 2) and probing H_2O_2 levels in chemotherapy treated rats (Chapter 3). Chapter 2 describes the fabrication process

and the characterization of the GO/Nafion CFME, as well as application of this sensor to measuring transient H_2O_2 concentrations in brain slices. Chapter 3 addresses post chemotherapy cognitive impairment (PCCI), also known as chemo brain. The symptoms of PCCI, plausible causes of PCCI, and measurements of H_2O_2, are also discussed. Finally, future directions and conclusions are presented in Chapter 4.

References

1. Kandel, E. R.; Schwartz, J. H.; Jessell, T. M.; Siegelbaum, S. A.; Hudspeth, A. J., *Principles of neural science*. 5th ed.; McGraw-Hill: New York, 2000.

2. Lovinger, D. M., Communication networks in the brain neurons, receptors, neurotransmitters, and alcohol. *Alcohol Research & Health* **2008,** *31* (3), 196-214.

3. Spanos, M.; Gras-Najjar, J.; Letchworth, J. M.; Sanford, A. L.; Toups, J. V.; Sombers, L. A., Quantitation of hydrogen peroxide fluctuations and. *ACS Chem. Neurosci.* **2013,** *4* (5), 782-789.

4. Cepeda, C.; Murphy, K. P.; Parent, M.; Levine, M. S., The role of dopamine in huntington's disease. *Prog. Brain Res.* **2014,** *211*, 235-254.

5. Dobryakova, E.; Genova, H. M.; DeLuca, J.; Wylie, G. R., The dopamine imbalance hypothesis of fatigue in multiple sclerosis and other neurological disorders. *Front. Neurol.* **2015,** *6*.

6. Rice, M. E., H2o2: A dynamic neuromodulator. *Neuroscientist* **2011,** *17* (4), 389-406.

7. Patel, J. C.; Rice, M. E., Classification of h(2)o(2)as a neuromodulator that regulates striatal dopamine release on a subsecond time scale. *ACS Chem. Neurosci.* **2012,** *3* (12), 991-1001.

8. Garris, P. A.; Wightman, R. M., Different kinetics govern dopaminergic transmission in the amygdala, prefrontal cortex, and striatum: An in vivo voltammetric study. *J. Neurosci.* **1994,** *14* (1), 442-450.

9. Garris, P. A.; Collins, L. B.; Jones, S. R.; Wightman, R. M., Evoked extracellular dopamine in vivo in the medial prefrontal cortex. *J. Neurochem.* **1993,** *61* (2), 637-647.

10. Suaud-Chagny, M. F.; Cespuglio, R.; Rivot, J. P.; Buda, M.; Gonon, F., High sensitivity measurement of brain catechols and indoles in vivo using electrochemically treated carbon-fiber electrodes. *J. Neurosci. Methods* **1993,** *48* (3), 241-250.

11. Scanziani, M.; Hausser, M., Electrophysiology in the age of light. *Nature* **2009,** *461* (7266), 930-939.

12. Michael, A. C.; Borland, L. M.; Editors, *Electrochemical methods for neuroscience*. CRC Press LLC: 2007; p 512 pp.

13. Kawagoe, K. T.; Garris, P. A.; Wiedemann, D. J.; Wightman, R. M., Regulation of transient dopamine concentration gradients in the microenvironment surrounding nerve terminals in the rat striatum. *Neuroscience* **1992,** *51* (1), 55-64.

14. Robinson, D. L.; Hermans, A.; Seipel, A. T.; Wightman, R. M., Monitoring rapid chemical communication in the brain. *Chem. Rev.* **2008,** *108* (7), 2554-2584.

15. Heien, M. L.; Johnson, M. A.; Wightman, R. M., Resolving neurotransmitters detected by fast-scan cyclic voltammetry. *Anal. Chem.* **2004,** *76* (19), 5697-5704.

16. Bard, A. J.; Faulkner, L. R., *Electrochemical methods: Fundamentals and applications*. 2nd ed.; John Wiley: New York, 2001.

17. Mosharov, E. V.; Sulzer, D., Analysis of exocytotic events recorded by amperometry. *Nat. Methods* **2005,** *2* (9), 651-658.

18. Leszczyszyn, D. J.; Jankowski, J. A.; Viveros, O. H.; Diliberto, E. J., Jr.; Near, J. A.; Wightman, R. M., Secretion of catecholamines from individual adrenal medullary chromaffin cells. *Journal of neurochemistry* **1991,** *56* (6), 1855-1863.

19. Kissinger, P. T.; Heineman, W. R., *Laboratory techniques in electroanalytical chemistry; revised and expanded*. 2 nd ed.; Marcel Dekker: New York, 1996.

20. Bard, A. J.; Faulkner, L. R., *Electrochemical methods: Fundamentals and applications*. Wiley: 1980; p 718 pp.

21. Millar, J.; Stamford, J. A.; Kruk, Z. L.; Wightman, R. M., Electrochemical, pharmacological and electrophysiological evidence of rapid dopamine release and removal in the rat caudate nucleus following electrical stimulation of the median forebrain bundle. *Eur. J. Pharmacol.* **1985,** *109* (3), 341-348.

22. Bull, D. R.; Palij, P.; Sheehan, M. J.; Millar, J.; Stamford, J. A.; Kruk, Z. L.; Humphrey, P. P., Application of fast cyclic voltammetry to measurement of electrically evoked dopamine overflow from brain slices in vitro. *J. Neurosci. Methods* **1990,** *32* (1), 37-44.

23. Wightman, R. M., Probing cellular chemistry in biological systems with microelectrodes. *Science (Washington, DC, U. S.)* **2006,** *311* (5767), 1570-1574.

24. Robinson, D. L.; Venton, B. J.; Heien, M. L.; Wightman, R. M., Detecting subsecond dopamine release with fast-scan cyclic voltammetry in vivo. *Clin. Chem.* **2003,** *49* (10), 1763-1773.

25. Wipf, D. O.; Kristensen, E. W.; Deakin, M. R.; Wightman, R. M., Fast-scan cyclic voltammetry as a method to measure rapid, heterogeneous electron-transfer kinetics. *Anal. Chem.* **1988,** *60* (4), 306-310.

26. Venton, B. J.; Michael, D. J.; Wightman, R. M., Correlation of local changes in extracellular oxygen and ph that accompany dopaminergic terminal activity in the rat caudate-putamen. *Journal of neurochemistry* **2003,** *84* (2), 373-381.

27. Bunin, M. A.; Wightman, R. M., Quantitative evaluation of 5-hydroxytryptamine (serotonin) neuronal release and uptake: An investigation of extrasynaptic transmission. *The Journal of neuroscience : the official journal of the Society for Neuroscience* **1998,** *18* (13), 4854-4860.

28. Park, J.; Takmakov, P.; Wightman, R. M., In vivo comparison of norepinephrine and dopamine release in rat brain by simultaneous measurements with fast-scan cyclic voltammetry. *Journal of neurochemistry* **2011,** *119* (5), 932-944.

29. Kaplan, S. V.; Limbocker, R. A.; Gehringer, R. C.; Divis, J. L.; Osterhaus, G. L.; Newby, M. D.; Sofis, M. J.; Jarmolowicz, D. P.; Newman, B. D.; Mathews, T. A.; Johnson, M. A., Impaired brain dopamine and serotonin release and uptake in wistar rats following treatment with carboplatin. *ACS Chem. Neurosci.* **2016,** *7* (6), 689-699.

30. Ross, A. E.; Venton, B. J., Nafion-cnt coated carbon-fiber microelectrodes for enhanced detection of adenosine. *Analyst* **2012,** *137* (13), 3045-3051.

31. Sanford, A. L.; Morton, S. W.; Whitehouse, K. L.; Oara, H. M.; Lugo-Morales, L. Z.; Roberts, J. G.; Sombers, L. A., Voltammetric detection of hydrogen peroxide at carbon fiber microelectrodes. *Anal. Chem.* **2010,** *82* (12), 5205-5210.

32. Ponchon, J. L.; Cespuglio, R.; Gonon, F.; Jouvet, M.; Pujol, J. F., Normal pulse polarography with carbon fiber electrodes for in vitro and in vivo determination of catecholamines. *Anal. Chem.* **1979,** *51* (9), 1483-1486.

33. Gonon, F.; Buda, M.; Cespuglio, R.; Jouvet, M.; Pujol, J. F., In vivo electrochemical detection of catechols in the neostriatum of anaesthetized rats: Dopamine or dopac? *Nature* **1980,** *286* (5776), 902-904.

34. McCreery, R. L., Advanced carbon electrode materials for molecular electrochemistry. *Chem. Rev.* **2008,** *108* (7), 2646-2687.

35. Cahill, P. S.; Walker, Q. D.; Finnegan, J. M.; Mickelson, G. E.; Travis, E. R.; Wightman, R. M., Microelectrodes for the measurement of catecholamines in biological systems. *Anal. Chem.* **1996,** *68* (18), 3180-3186.

36. Pons, S.; Fleischmann, M., The behavior of microelectrodes. *Anal. Chem.* **1987,** *59* (24), A1391-A1399.

37. Shin, M.; Kaplan, S. V.; Raider, K. D.; Johnson, M. A., Simultaneous measurement and quantitation of 4-hydroxyphenylacetic acid and dopamine with fast-scan cyclic voltammetry. *Analyst* **2015,** *140* (9), 3039-3047.

38. Bartlett, P. N.; Cooper, J. M., A review of the immobilization of enzymes in electropolymerized films. *J. Electroanal. Chem.* **1993,** *362* (1-2), 1-12.

39. Bledsoe, J. M.; Kimble, C. J.; Covey, D. P.; Blaha, C. D.; Agnesi, F.; Mohseni, P.; Whitlock, S.; Johnson, D. M.; Horne, A.; Bennet, K. E.; Lee, K. H.; Garris, P. A., Development of the wireless instantaneous neurotransmitter concentration system for intraoperative neurochemical monitoring using fast-scan cyclic voltammetry. *J. Neurosurg.* **2009,** *111* (4), 712-723.

40. Murray, R. W., Chemically modified electrodes for electrocatalysis. *Philosophical Transactions of the Royal Society a-Mathematical Physical and Engineering Sciences* **1981,** *302* (1468), 253-265.

41. Wang, J., Modified electrodes for electrochemical sensors. *Electroanalysis* **1991,** *3* (4-5), 255-259.

42. Shahrokhian, S.; Naderi, L.; Ghalkhani, M., Modified glassy carbon electrodes based on carbon nanostructures for ultrasensitive electrochemical determination of furazolidone. *Mater. Sci. Eng., C* **2016,** *61*, 842-850.

43. Ustundag, I.; Erkal, A.; Koralay, T.; Kadioglu, Y. K.; Jeon, S., Gold nanoparticle included graphene oxide modified electrode: Picomole detection of metal ions in seawater by stripping voltammetry. *J. Anal. Chem.* **2016,** *71* (7), 685-695.

44. Zestos, A. G.; Jacobs, C. B.; Trikantzopoulos, E.; Ross, A. E.; Venton, B. J., Polyethylenimine carbon nanotube fiber electrodes for enhanced detection of neurotransmitters. *Anal. Chem.* **2014,** *86* (17), 8568-8575.

45. Molina, J.; Fernandez, J.; Cases, F., Scanning electrochemical microscopy for the analysis and patterning of graphene materials: A review. *Synth. Met.* **2016,** *222* (Part_B), 145-161.

46. Bai, J.; Wu, L.; Wang, X.; Zhang, H.-M., Hemoglobin-graphene modified carbon fiber microelectrode for direct electrochemistry and electrochemical h2o2 sensing. *Electrochim. Acta* **2015,** *185*, 142-147.

47. Taylor, I. M.; Robbins, E. M.; Catt, K. A.; Cody, P. A.; Happe, C. L.; Cui, X. T., Enhanced dopamine detection sensitivity by pedot/graphene oxide coating on in vivo carbon fiber electrodes. *Biosens. Bioelectron.* **2017,** *89* (Pt 1), 400-410.

Chapter 2: A graphene modified electrode for measuring hydrogen peroxide

1. Introduction

1.1 Hydrogen peroxide.

Hydrogen peroxide (H_2O_2) is a reactive oxygen species and membrane-permeable neuromodulator produced naturally in cells. It is among the most stable ROS, with a half-life of 10^{-5} sec,[1] and hence plays a crucial role in numerous physiological processes, both inter- and intra-cellularly. For example, H_2O_2 signaling plays a role in the local regulation of DA release in the striatum in a mechanism first involving the activation of AMPA receptors, located on medium spiny neurons (MSNs), by glutamate. This activation is followed by production of H_2O_2 in the mitochondria of MSNs and its subsequent diffusion to K^+_{ATP} channels, located on dopaminergic terminals. These channels are then modified to allow the passage of potassium ion (K^+) into the cell, thereby inhibiting dopamine release.[2] In addition to its role as a neuromodulator, H_2O_2 has practical uses. For example, enzymatically generated H_2O_2 has been used as a reporter molecule generated by oxidase enzymes, such as glutamate oxidase and glucose oxidase,[3, 4] at enzyme-modified microelectrodes that are used to monitor non-electroactive species, such as glutamate and glucose.[4] In its capacity as an ROS, H_2O_2 forms hydroxyl radicals that can irreversibly alter the structure of DNA, lipids, and proteins, resulting in pathological oxidative stress, neuronal degeneration, and aging.[4-6] Therefore, given its biological importance, the quantitative measurement of H_2O_2 levels in tissues, especially those that are richly oxygenated such as the brain, would be useful for understanding neuronal function and resolving disease mechanisms.

Cellular Production of Hydrogen Peroxide

Although H_2O_2 may be formed by multiple mechanisms, three of the most prominent modes of formation include mitochondrial respiration and metabolic reactions involving either monoamine oxidase (MAO) or NADPH Oxidase (Nox).[2, 7]

Mitochondrial Respiration. Mitochondrial respiration is thought to be the primary production source of H_2O_2 that participates in the modulation of dopamine. Here, O_2 is reduced to form the superoxide ion and it is converted to H_2O_2 by superoxide dismutase (SOD). Four sub complexes are included in the mitochondrial electron transport chain (I- IV). Super oxide ion ($O_2^{\cdot -}$) is mainly generated in complex I and III.[8]

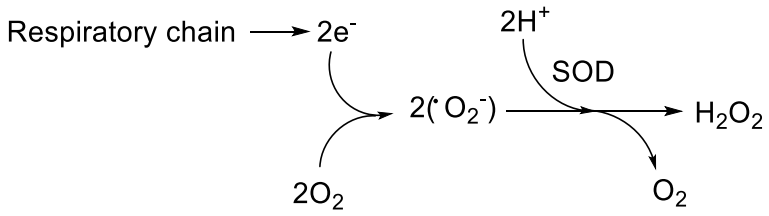

Scheme 1. Generation of H_2O_2 in the respiratory chain

Monoamine Oxidase. MAO controls monoamine levels by catalyzing oxidative deamination of monoamines.[9, 10] Monoamine neurotransmitters are involved in cognitive function. Hence, excessive levels of monoamines can lead to several neurological disorders. MAO is essential in controlling the monoamine levels. This enzyme, which is abundant in the striatum as well as other brain regions that have high concentrations of catecholamines, catalyzes the deamination of DA by a two-electron reduction of O_2 to form H_2O_2.[9]

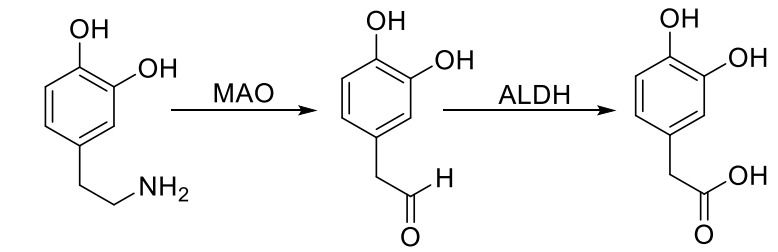

Dopamine (DA) 3,4-Dihydroxyphenyl-3-acetaldehyde (DOPAL) 3,4-Dihydroxyphenylacetic acid (DOPAC)

A

Scheme 2. Deamination of DA[10]

NADPH Oxidase. NADPH Oxidase (Nox) enzymes catalyze the one electron reduction of O_2 to form super oxide ion and subsequently form H_2O_2. Nox can be found in striatum and a variety of signaling pathways[11-14] Moreover, enzymes in mitochondria such as NADPH, Xanthine Oxidase (XO) and Cytochrome p-450 reductase can convert anthracyclines to quinone or semiquinone through one electron reduction of the quinone moiety. Resulting semiquinones can be converted back to quinone by reacting with O_2 producing super oxide anion which is eventually converted in to H_2O_2. Some chemotherapeutic drugs such as doxorubicin can increase ROS production via this process.[11]

1.2 Electrodes for the detection of hydrogen peroxide

Historically, platinum electrodes have been useful in the detection of H_2O_2 given its ability resist chemical reactions and oxidize H_2O_2 at low applied potentials.[15] For instance, George Wilson and coworkers have studied electrochemical oxidation of H_2O_2 on Pt and Pt/Ir electrodes with amperometry, in which the electrodes were held a constant potential of 0.65 V vs Ag/AgCl reference electrode.[4, 16] More recently, FSCV at bare carbon-fiber microelectrodes has been used to detect H_2O_2 in brain tissues.[2] This adaptation has provided a method to monitor

transient changes in H_2O_2 levels, on the sub-second timescale, in the rodent brain *in vivo*[17] and *ex vivo*.[2]

$$H_2O_2 \longrightarrow O_2 + 2H^+ + 2e^-$$

Equation 1. Irreversible oxidation of H_2O_2

Despite the utility of these electrode materials in detecting H_2O_2, progress is hampered by the fact that extracellular levels are low (in the µM range), making it difficult to detect without pharmacological intervention, such as addition of mercaptosuccinic acid, a peroxidase inhibitor. For this reason, we explored electrode modifications that might improve limits of detection for H_2O_2. Several types of modifications to carbon-fiber microelectrodes have been used to enhance the detection of various analytes. For example, Nafion, a negatively charged, water permeable fluoropolymer that hinders access of anions to the electrode surface,[18] has been used to improve the detection of catecholamines while suppressing interference from negatively charged species, such as ascorbate.[18, 19] Other modifications have also been combined with Nafion and other polymers to selectively improve the signal. For example, carbon nanotubes, in conjunction with other polymers, such as poly (3,4ethelenethiophene)PEDOT,[20] have been adsorbed to the surface to enhance detection of dopamine and octopamine in fruit flies.[21]

1.3. Electrode modification with graphene oxide

While the most common carbon-based modifications used in the past have been carbon nanotubes (CNT) and multiwalled carbon nanotubes (MWNT), graphene oxide (GO) has gained recent attention due to beneficial characteristics, including electrical, conductivity, thermal, mechanical and chemical properties,[22, 23] that enhance detection of specific analytes.[20,24-26] GO possesses a 2-dimensional honeycomb structure consisting of sp^2- and sp^3-hybridized carbon atoms functionalized with epoxide, hydroxyl, carbonyl and carboxylic (Fig. 1).[22,27] These

structural features provide several advantages. First, the presence of functional groups facilitate the dispersal of GO in water and many organic solvents. Also, oxygen molecules in GO facilitate immobilization of the nanoparticles on electrode surfaces.[27, 28] Furthermore, its 2D lattice structure provides a large platform for loading nanoparticles which effectively increases the surface area of the microelectrode. Finally, GO can be prepared easily from graphite using the Hummers method and GO can be considered as a precursor for graphene and reduced graphene oxide (rGO). Recently, graphene modified microelectrodes have been used for the detection of dopamine in the brain.[20, 26] In this work, we have modified carbon-fiber microelectrodes by dip-coating in a graphene oxide slurry, followed by electrodeposition of Nafion onto the surface. We have found that this modification improved the sensitivity to H_2O_2 more than five-fold while having little effect on the detection of dopamine and serotonin. This electrode modification could improve the capability of selectively detecting H_2O_2 in the brain.

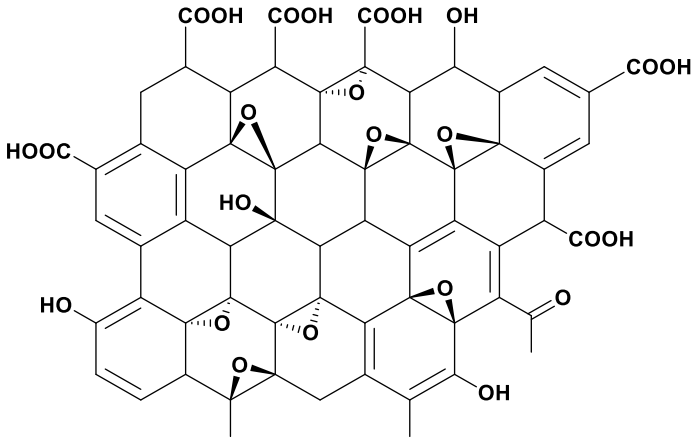

Figure 1. Structure of graphene[22]

2. Experimental Procedures

2.1 Chemicals

Graphene oxide (2mg/ml) in H_2O, lot# 763765, 25ml and all other chemicals were purchased from Sigma – Aldrich (St. Louis, MO, USA) and used as received, unless otherwise noted. Physiologically buffered artificial cerebrospinal fluid (aCSF) buffer solution, used in all flow injection analysis measurements, consisted of (in mM): 126 NaCl, 2.5 KCl, 25 $NaHCO_3$, 1.2 NaH_2PO_4, 2.4 $CaCl_2$, 1.2 $MgCl_2$, 20 HEPES and was adjusted to a pH of 7.4. All aqueous solutions were prepared with ultra-pure MilliQ (18.2 MΩ) water.

2.2 Fabrication of GO/Nafion/CFME

Carbon-fiber microelectrodes were made in-house. A 7 µm carbon fiber was loaded into glass capillaries by aspiration (4 in, 1.2Cmm OD; A-M System, Inc. Carlsberg, WA, USA) and capillaries were pulled using a heated coil puller (Narishige International USA, East Meadow, NY, USA). Carbon-fiber tips were then cut, with a scalpel, so that the exposed electroactive surface projected 50 µm from the end of the glass seal. Electrodes were sealed using an epoxy mixture of 0.24 grams EPI-CURE 3234 Curing Agent and 2.00 grams EPON Resin 815C. Excess resin was removed by dipping the electrodes several times in toluene. Finally, the electrodes were baked for 1 hour at 100 °C. The electrodes were back filled with 0.5 M potassium acetate in order to establish an electrical connection. Prepared CFMEs were modified as follows. First, CFMEs were dip-casted with 1 mg/ml GO suspension and air dried over night to prepare the GO/CFME. Ultra-pure Milli-Q water (18.2 MΩ) was used in preparation of 1 mg/ml GO from the 2 mg/ml GO commercially provided suspension. Second, 5% Nafion solution in methanol was electrochemically deposited on the GO casted carbon fiber microelectrodes (+1.0 V for 30 seconds, and oven baked at 70°C for 10 min).[29]

2.3 Characterization of the electrode surface

Electrode surface characterization was carried out in the University of Kansas Microscopy and Analytical Imaging Laboratory. The surface of the modified carbon-fiber was characterized using a VERSA 3D dual beam Scanning electron microscope FEI (Abingdon, Oxford Shire, United Kingdom). Moreover, composition of the modified electrode surface was studied using (EDX) energy dispersive X-ray spectroscopy (Oxford Instruments X- Max^{N}) 10keV, resolution width 512 pixel, resolution height 352 pixel, Magnification 30,000X.

2.4 Flow cell analysis for the modified electrodes.

The electrochemical characteristics of the modified electrode, referenced against a Ag/AgCl electrode, was studied by flow injection analysis at room temperature. The workstation consisted of a Chem-Clamp potentiostat (Dagan Corp., Minneapolis, MN) interfaced with a personal computer by a locally constructed breakout box. Tar Heel Software (M. Heien and R.M. Wightman, University of North Carolina, Chapel Hill) was used. Figure 2 shows a schematic diagram of the flow injection analysis system. A 6-port Rheodyne-type HPLC valve was used to control the introduction of analyte to the working electrode through the sample loop.

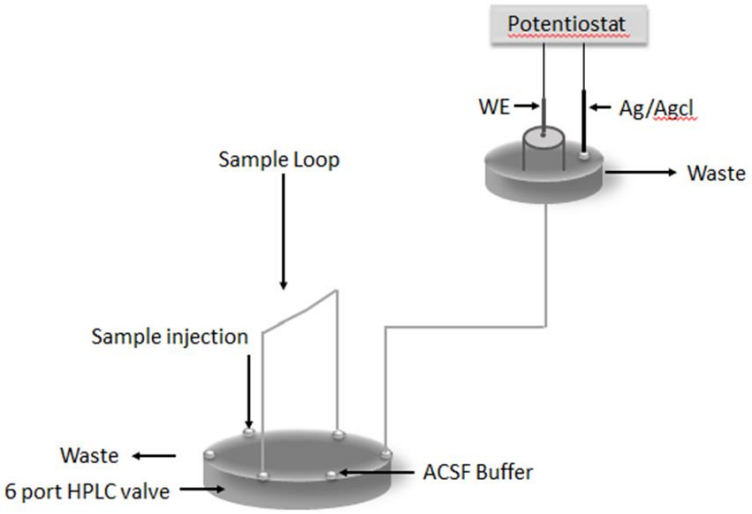

Figure 2. Schematic diagram of the injection analysis system (where, WE = working electrode, RE = reference electrode

A syringe pump supplied the aCSF buffer from a 50 mL syringe at a flow rate of 1 ml/min across the working electrode. Analyte was introduced to the working electrode through a sample loop with a Rheodyne-type valve. Analyses were performed separately for hydrogen peroxide (H_2O_2), dopamine (DA), and serotonin (5-HT). During each injection, a triangular waveform of -0.4V to 1.4V to -0.4V was applied to the working electrode at a scan rate of 400 V/s and an update rate of 10 CVs/s. A background CV, obtained by averaging 10 CVs collected prior to the injection of analyte, was subtracted from the entire set of CVs collected for each file (20 to 30 s in duration). This background subtraction process eliminates the large non-faradaic charging current observed at high scan rates.[30] During collection, data were treated with a 3 kHz low-pass filter (from the Dagan Chem-Clamp). Analyzed color plot data were treated with a 2 kHz low-pass filter in the Tar Heel data analysis program.

2.5 Statistics

Statistically significant differences were determined using student's t tests and ANOVA tests with *post hoc* analysis. A value of $p < 0.05$ was used to delineate statistical significance. The limit of detection (LOD) was defined as three times the noise (S/N = 3) and the limit of quantitation was defined at ten times the noise (S/N = 10). GraphPad Prism 5.1 (GraphPad Software, Inc, La Jolla, CA) was used for graphical presentation and statistical analysis.

3. Results and Discussion

3.1 Characterization of electrode surface (Bare Vs Modified)

The morphology of the modified carbon fiber was investigated by scanning electron microscopy (SEM). Figure 3A shows an SEM image of an unmodified carbon-fiber whereas Figure 3B shows an SEM image of a carbon-fiber microelectrode modified with GO/Nafion. As can be seen, the coated electrode appears to have a thin film of Nafion and GO adsorbed to the surface. To confirm further the presence of GO, energy dispersive X-ray spectroscopy (EDX) analysis was also performed on the electrode surfaces. This method of analysis identifies the presence of functional groups by ejecting inner shell electrons, induced by exposure to an X-ray beam, and the subsequent release of X-rays from the sample. The energy of the emitted X-ray is characteristic of the exposed element.

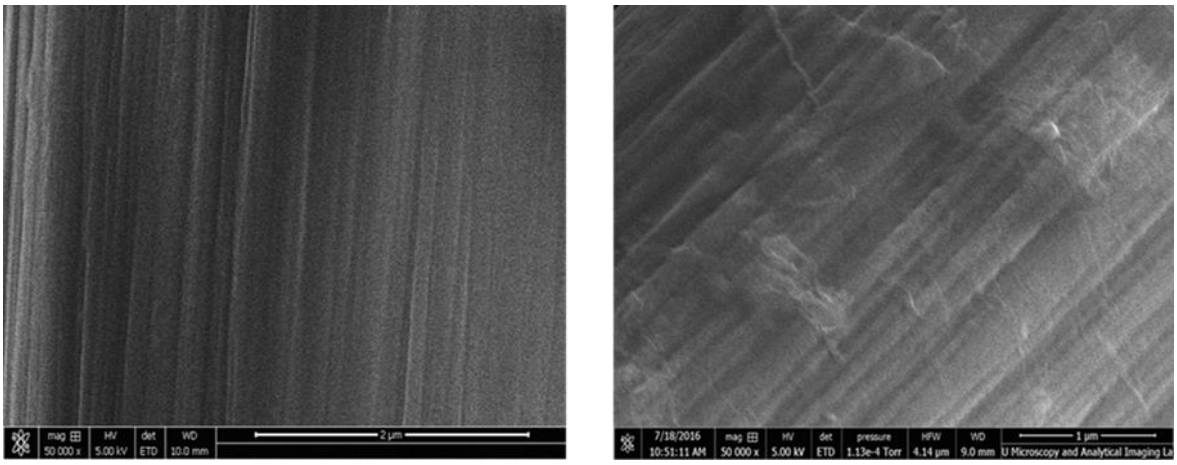

A **B**

Figure 3. SEM image of unmodified carbon-fiber microelectrode (A) and GO/Nafion coated carbon-fiber (B). Magnification: 50,000X.

Resulting spectra for both the bare and modified electrode are shown in Figure 4. In the case of the bare electrode (Figure 4A), a single, large peak was observed at an intensity of

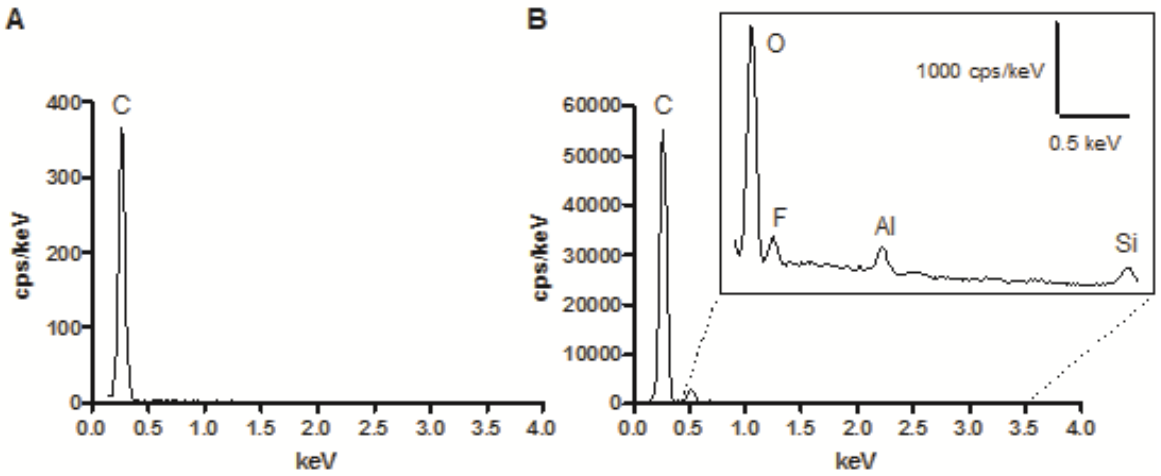

Figure 4. (A) EDX spectrum of bare CF (B) EDX spectrum of GO/Nafion CF. Labels: C, carbon; O, oxygen; F, fluorine; Al, aluminum; Si, silicon.

about 360 cps/keV, indicating primarily the presence of carbon. On the other hand, analysis of the modified electrode (Figure 4B) revealed multiple peaks. The carbon peak was present at much greater intensity (55,000 cps/keV). Additionally, smaller peaks for oxygen (500 cps/keV) and fluorine (650 cps/keV) were also present. These peaks likely indicate the presence of graphene oxide, which contains carbon and oxygen groups, and also Nafion, which contains carbon and fluorine. Although it is not clear why peaks at ~1.6 and ~3.1 are present, it is likely they arise from Al and Si contamination. Collectively, these results suggest that graphene oxide and Nafion were effectively immobilized on the surface of the electrode.

3.2. Electrochemical analysis of modified electrodes

The next step was to electrochemically characterize the modified electrode for comparison with the bare carbon-fiber microelectrode. A flow injection analysis system, in which

the microelectrodes were exposed to analyte by injection through a sample loop under control of a Rheodyne-type valve, was used. A sample file, obtained by a single injection of H_2O_2 at a concentration of 10 µM, is shown in Figure 5A. The CV reveals an irreversible oxidation reaction occurring, with the oxidation peak occurring at about +1.2 V on the backsweep,[32] after the potential had already reached the maximum of +1.4 V. A similar peak was observed when measuring H_2O_2 with bare carbon-fiber microelectrodes Figure 5B.[31] The signal increased from 10 to 90% in 2 ± 0.2 seconds for the modified electrode, compared to 2.5 ± 0.3 seconds for the bare electrode ($p > 0.05$, student's t-test, $n = 4$,). Thus, the modification appears to not significantly alter the kinetics of the oxidation reaction.

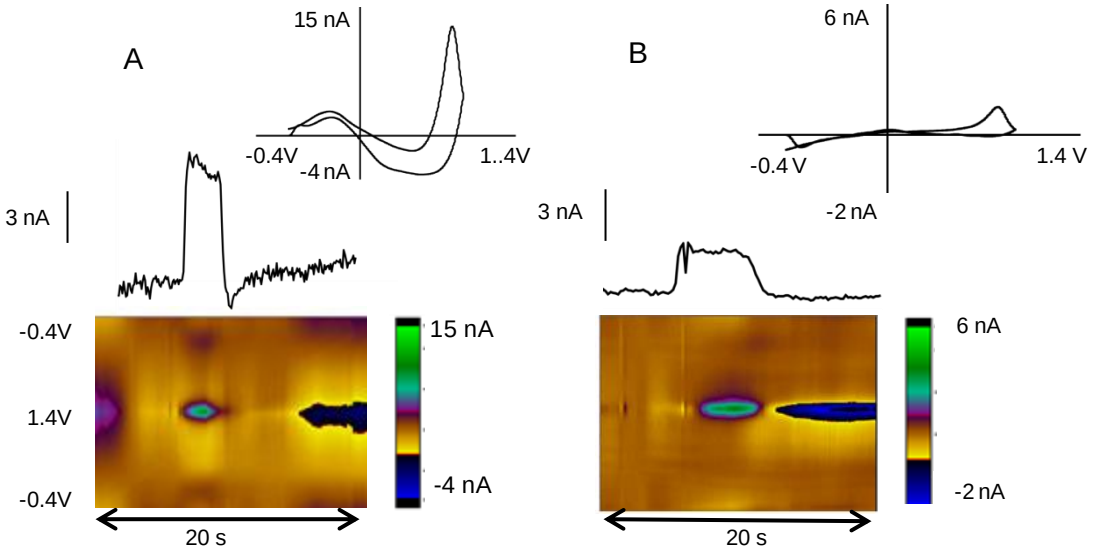

Figure 5. Detection of H_2O_2 oxidation in a flow injection analysis system (A) with GO/Nafion CFME , (B) with bare CFME.

The oxidation currents and cyclic voltammograms of bare electrodes, Nafion-coated electrodes, and Nafion/GO modified electrodes, obtained by flow cell analysis, were compared

(Figure 6). Oxidation currents obtained for the modified electrode were enhanced 5.3 fold compared to the bare carbon-fiber microelectrode (n = 6 for bare and modified, n = 3 for Nafion, ANOVA $p < 0.05$). An irreversible oxidation peak was observed at about 1.2 V,[31] for the bare and Nafion-coated carbon fiber micro electrodes. The oxidation peak (Ep) for the modified electrode was shifted towards a positive potential (about +0.1 V) on the backsweep.

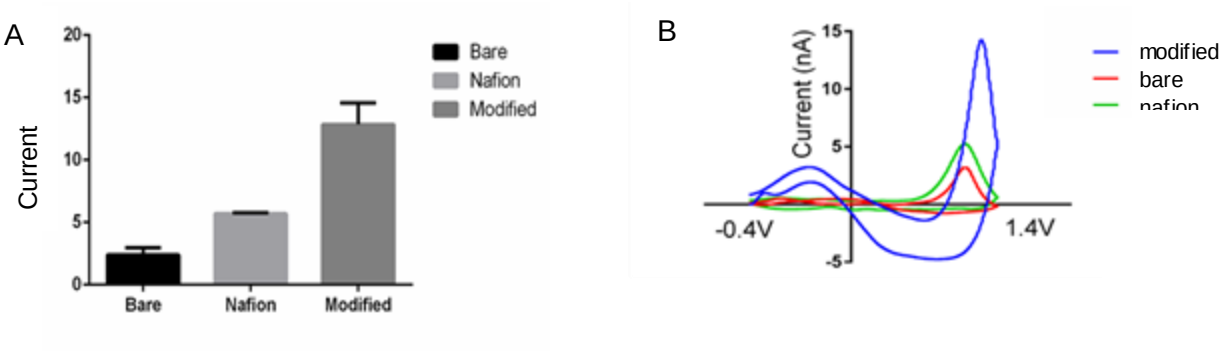

Figure 6. (A) Comparison data for oxidation current for H_2O_2 obtained with bare, Nafion coated and GO/Nafion coated CF micro electrodes. (B) Comparison cyclic voltammograms. Oxidation current for H_2O_2 is significantly increased 5.3 fold enhancement

Representative data for the electrochemical characteristics of the modified electrode for dopamine and serotonin are shown in Figure 7. Obtained CVs were very similar to those obtained with bare carbon-fiber electrodes. The dopamine oxidation peak occurred at +0.6V whereas the reduction peak occurred at -0.2V. For serotonin, the oxidation peak was observed around +0.8V and the reduction peak was observed -0.15V. Moreover, for Dopamine, a 2.1 fold enhancement in the current was obtained compared to the bare electrode (3 µM, Dopamine, n =

4 electrodes, t test p<0.05). However, current enhancement for the serotonin was not increased significantly (2 µM, serotonin, n = 3, t-test, P>0.05, not significant).

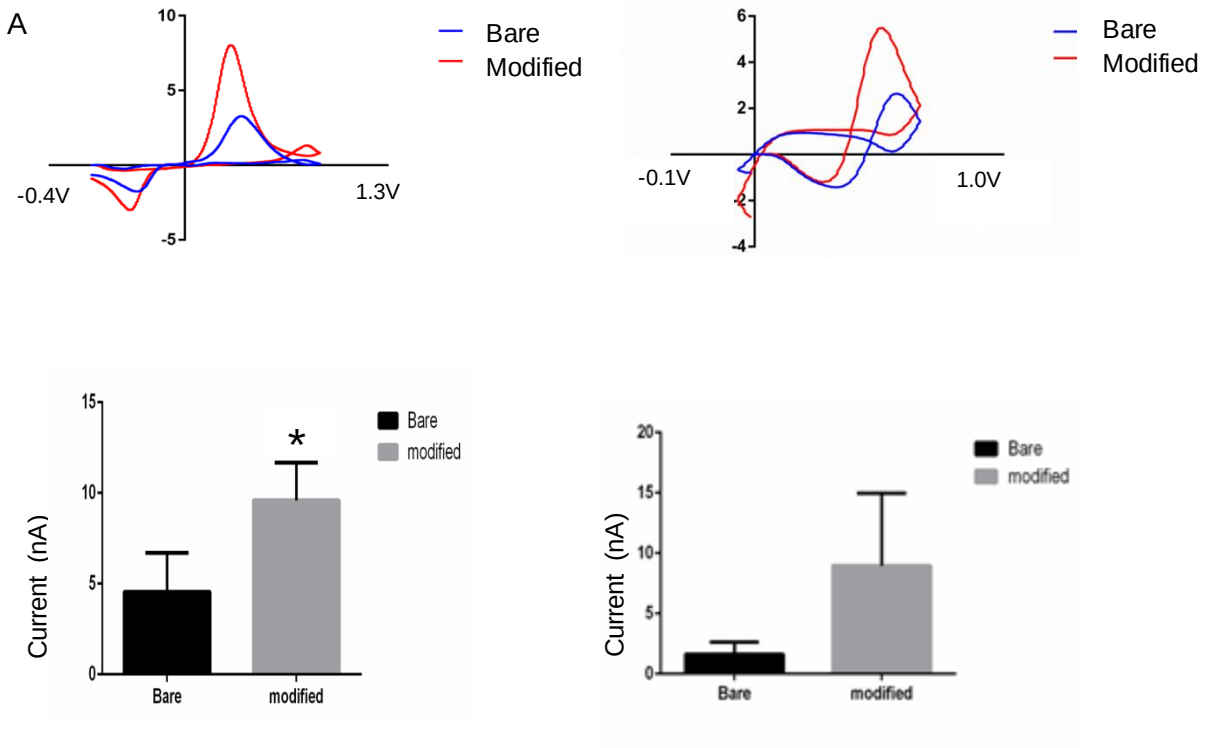

For 3 µM, Dopamine (n=4), t test P<0.05

For 2 µM, Serotonin (n=3), t-test, P>0.05, not significant

Figure 7. Electrochemical response of the modified electrode towards (A) dopamine (3 µM) and (B) serotonin (2 µM).

3.3. Stability

For obtaining consistent data the currents obtained with the modified electrode should not change with the time. Stability of the Current for the modified electrode was studied over one hour for 5 µM H_2O_2. This time frame is generally consistent with the amount of time needed to

obtain a set of measurements in a brain slice. The current was found to be stable for the

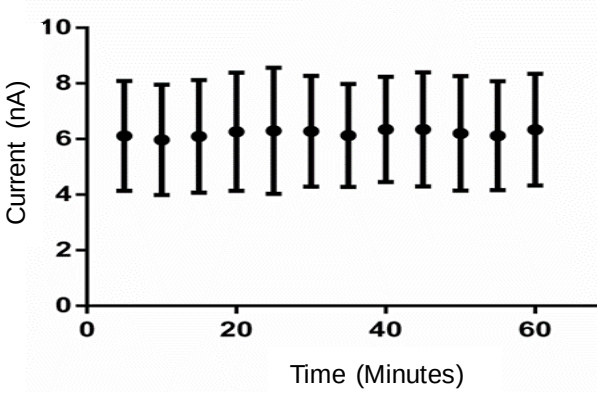

GO/Nafion CFME during this time (Figure 8).

Figure 8. Stability test. Electrode response to injection of 5 µM H_2O_2 was measured over a one hour period. Peak current did not deviate significantly over time. N = 3 electrodes.

Obtaining a stable current is essential for modified electrodes since most of the time modified electrodes can be foul. Modified materials can be delaminate from the electrode surface when used in aqueous solutions for a longer time. To prevent electrode fouling and to obtain a long lasting electrode, researchers often use conductive polymers such as PEDOT and Nafion. In addition to the prevention of electrode fouling these conductive polymers can exclude interfering ions.[15] For instance, Nafion which is a cationic exchange polymer can exclude negatively charged ions.

Obtaining a thin coating of these conductive polymers can be controlled by applying a potential which is sufficient to oxidize and polymerize the polymer. Moreover, incorporating negatively charged GO in to a conductive polymer allows it to be used as an electrode material without losing the conductivity.[20]

3.4. LOD/LOQ

Calibration curves for detection of H_2O_2 with bare and modified electrodes is shown in Figure 9. For bare electrodes, the current response to increasing H_2O_2 concentrations was linear up to about 100 µM (R^2 = 0.99, linear regression), while a deviation from linearity at 50 µM was noted for the modified electrode. It is not yet clear why this deviation from linearity occurs. Measurements obtained previously with bare carbon-fiber microelectrodes in anesthetized rats have measured H_2O_2 transients at a peak concentration of ~5 µM.[2] This concentration falls within the dynamic range of our GO/Nafion modified electrode. It must be mentioned, however, that, in the case of certain pathologies, such as global ischemia, H_2O_2 levels have been estimated to climb as high as 100 µM (outside the linear range); in this case, caution should be used in interpreting measurement results.

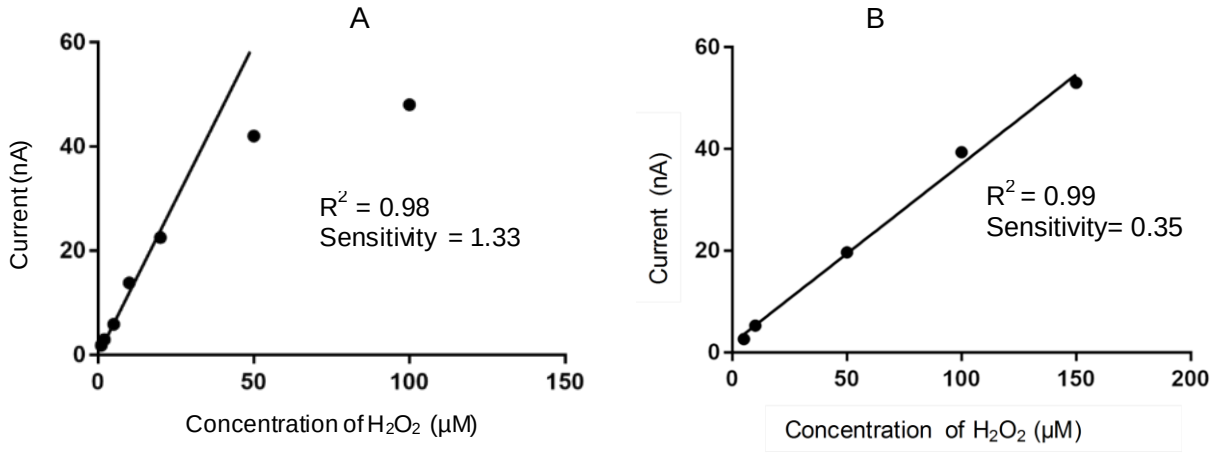

Figure 9. Calibration curves for modified (A) and bare (B) electrodes. Sensitivity is enhanced by 3.7 fold n = 3

The sensitivities, obtained from the slopes of the lines, were 0.352 nA/µM for the bare electrode and 1.33 nA/µM for the modified electrode. The limits of detection (LOD, based on

S/N=3) and quantitation (LOQ, based on S/N=10) for the bare electrode was 2500 nM, 8250 nM respectively, while that for the modified electrode was 50 nM and 165 nM. Thus, we found that, for detection of H_2O_2, the GO/Nafion treatment provided a 3.7 fold enhancement in sensitivity, and substantially improved LOD and LOQ. A similar enhancement sensitivity had previously been obtained by modifying carbon-fiber microelectrodes for the detection of neurotransmitters.

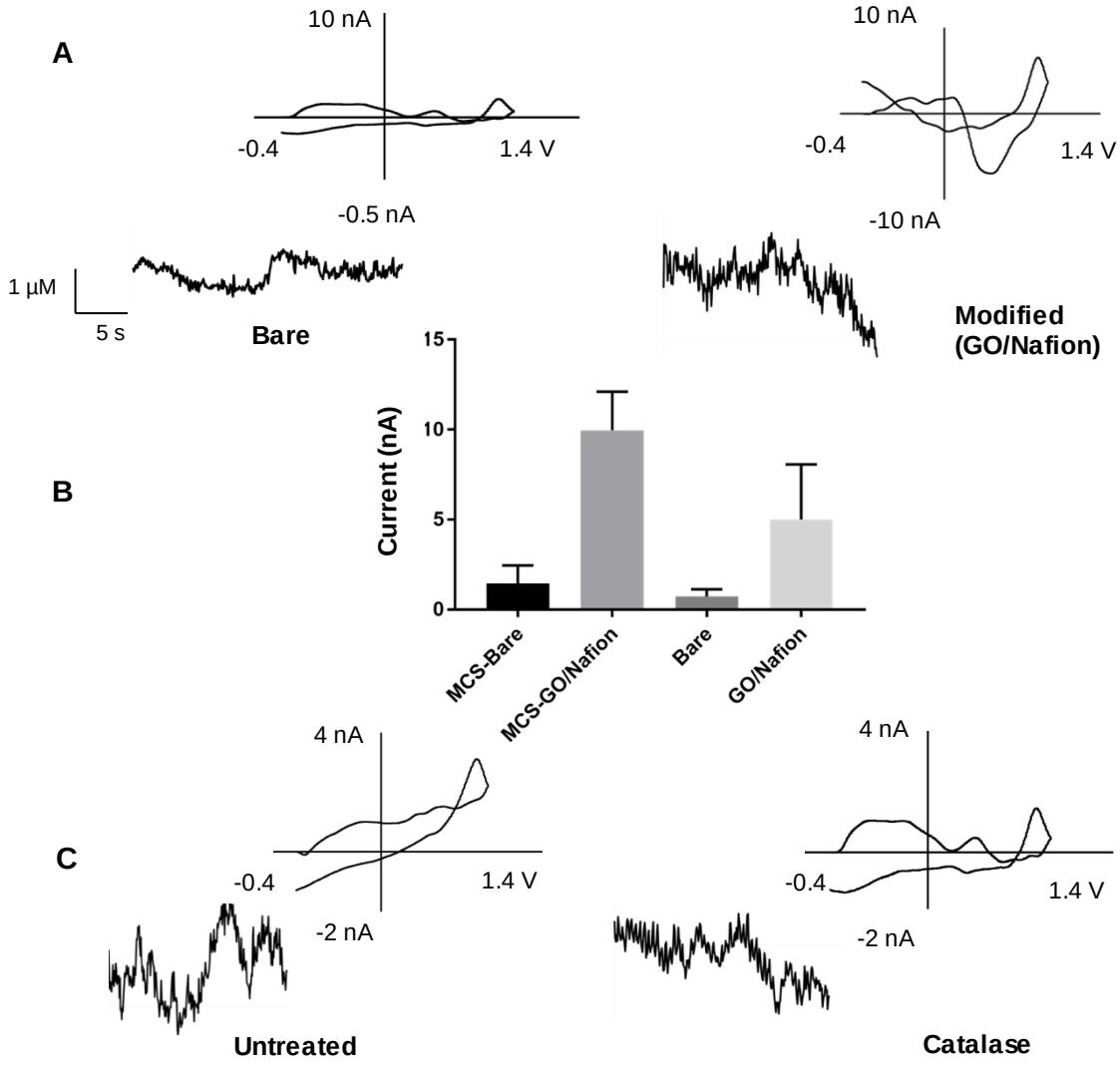

Figure 10. H_2O_2 release plot for Bare and GO/Nafion CFME(A), H_2O_2 transients in MCS treated and untreated rats with bare and GO/Nafion CFME (B), Decomposition of H_2O_2 upon the introduction of catalase(C).

These modifications include the use of graphene oxide with PEDOT for enhanced detection of dopamine (880% increase in sensitivity)[20] and carbon nanotubes with Nafion (2.3-fold increase in sensitivity). Our modified sensor provided roughly a two-fold enhancement in response to 3 μM dopamine and appeared to give a slightly enhanced response to 2 μM serotonin, although not statistically significant. Although the reason behind this selective enhancement of the H_2O_2 electrochemical response is not clear, it is possible that H_2O_2 being smaller and highly diffusible compared to dopamine and serotonin, is less impeded in traveling though the Nafion coating.

3.5. Brain slice studies. Given the positive results obtained for the detection of H_2O_2, our next step was to apply this electrode for the measurement of H_2O_2 in brain slices.[2] Shown in Figure 10 are data obtained from a striatal brain slice taken from a Sprague-Dawley rat. Figure 10A shows a representative H_2O_2 release plot and CV for bare and GO/Nafion coated electrodes. In this case, the slice was treated with MCS to enhance the formation of H_2O_2 transients. Also, results from MCS-treated and untreated slices are summarized in Figure 10B. From these data, it is apparent that the GO/Nafion coating significantly enhanced the H_2O_2 signal in both MCS-treated ($p<0.05$, t-test, N = 4 electrodes) and untreated ($p<0.05$, t-test, N = 4 electrodes) slices. Treatment of the slice with catalase (Figure 10C), an antioxidant enzyme that catalyzes the decomposition of H_2O_2 in to water and oxygen, decreased the current, measured with the GO/Nafion electrode, providing positive identification of H_2O_2. Therefore, we conclude that modification of the electrode surface with GO/Nafion improves the ability to detect H_2O_2 transients in striatal brain slices.

3.6 Conclusions

In this work, we have designed, constructed, and evaluated a novel graphene electrode for the detection of hydrogen peroxide. Morphological studies done with SEM revealed the thin coating of the GO/Nafion on the carbon fiber surface and the EDX spectrums confirmed the presence of

oxygen containing groups. Moreover, flow cell analysis with 10 µM H_2O_2 revealed that the oxidation current for the modified electrode was increased by 5.3 fold compared to the bare carbon-fiber micro electrode. Limit of detection of the GO/Nafion CFME was found to be 0.05 µM compared to 2.5 µM for the bare electrode and the sensitivity was found to be increased by 3.7 fold. Cyclic voltammograms, obtained using the modified electrode in a brain slice, were similar to that of the bare carbon-fiber microelectrodes, except for a ~0.1 V shift in oxidation peak to a more positive potential on the backsweep. Currents obtained from the oxidation of H_2O_2 (confirmed by addition of catalase) in brain striatal brain slices without MCS were greater when using the GO/Nafion modified electrode compared to the bare electrode, both in the absence of MCS and in the presence of MCS.

Acknowledgments

Dr Thapa Chetri premsingh, Scanning electron microscopy Lab, University of Kansas for help with electrode surface analysis.

Racheal Ginther for help with Chemotherapy treatments and anesthetizing and decapitating animals.

Funding

The University of Kansas

Institutional Development Award (IDeA) from the National Institute of General Medical Sciences of the National Institutes of Health under Award Number P20GM103638 (MAJ)

References

1. Giorgio, M.; Trinei, M.; Migliaccio, E.; Pelicci, P. G., Hydrogen peroxide: A metabolic by-product or a common mediator of ageing signals? *Nat. Rev. Mol. Cell Biol.* **2007,** *8* (9), 722-728.

2. Spanos, M.; Gras-Najjar, J.; Letchworth, J. M.; Sanford, A. L.; Toups, J. V.; Sombers, L. A., Quantitation of hydrogen peroxide fluctuations and their modulation of dopamine dynamics in the rat dorsal striatum using fast-scan cyclic voltammetry. *ACS Chem. Neurosci.* **2013,** *4* (5), 782-789.

3. Michael, A. C.; Borland, L. M.; Editors, *Electrochemical methods for neuroscience*. CRC Press LLC: 2007; p 512 pp.

4. Armstrong, F. A.; Wilson, G. S., Recent developments in faradaic bioelectrochemistry. *Electrochimica Acta* **2000,** *45* (15–16), 2623-2645.

5. Reczek, C. R.; Chandel, N. S., Ros-dependent signal transduction. *Curr. Opin. Cell Biol.* **2015,** *33*, 8-13.

6. Lennicke, C.; Rahn, J.; Lichtenfels, R.; Wessjohann, L. A.; Seliger, B., Hydrogen peroxide – production, fate and role in redox signaling of tumor cells. *Cell Commun Signal. CCS* **2015,** *13*.

7. Avshalumov, M. V.; Patel, J. C.; Rice, M. E., Ampa receptor-dependent h2o2 generation in striatal medium spiny neurons but not dopamine axons: One source of a retrograde signal that can inhibit dopamine release. *J. Neurophysiol.* **2008,** *100* (3), 1590-1601.

8. Lee, S.; Tak, E.; Lee, J.; Rashid, M.; Murphy, M. P.; Ha, J.; Kim, S. S., Mitochondrial h(2)o(2) generated from electron transport chain complex i stimulates muscle differentiation. *Cell Res.* **2011,** *21* (5), 817-834.

9. Edmondson, D. E.; Mattevi, A.; Binda, C.; Li, M.; Hubalek, F., Structure and mechanism of monoamine oxidase. *Curr. Med. Chem.* **2004,** *11* (15), 1983-1993.

10. Azzaro, A. J.; King, J.; Kotzuk, J.; Schoepp, D. D.; Frost, J.; Schochet, S., Guinea pig striatum as a model of human dopamine deamination: The role of monoamine oxidase isozyme ratio, localization, and affinity for substrate in synaptic dopamine metabolism. *J. Neurochem.* **1985,** *45* (3), 949-956.

11. Angsutararux, P.; Luanpitpong, S.; Issaragrisil, S., Chemotherapy-induced cardiotoxicity: Overview of the roles of oxidative stress. *Oxid. Med. Cell. Longev.* **2015,** *2015*, 795602.

12. Infanger, D. W.; Sharma, R. V.; Davisson, R. L., Nadph oxidases of the brain: Distribution, regulation, and function. *Antioxid. Redox Signal.* **2006,** *8* (9-10), 1583-1596.

13. Kishida, K. T.; Klann, E., Sources and targets of reactive oxygen species in synaptic plasticity and memory. *Antioxid. Redox Signal.* **2007,** *9* (2), 233-244.

14. Bao, L.; Avshalumov, M. V.; Patel, J. C.; Lee, C. R.; Miller, E. W.; Chang, C. J.; Rice, M. E., Mitochondria are the source of hydrogen peroxide for dynamic brain-cell signaling. *J. Neurosci.* **2009,** *29* (28), 9002-9010.

15. Roberts, J. G.; Hamilton, K. L.; Sombers, L. A., Comparison of electrode materials for the detection of rapid hydrogen peroxide fluctuations using background-subtracted fast scan cyclic voltammetry. *Analyst* **2011,** *136* (17), 3550-3556.

16. Zhang, Y.; Wilson, G. S., Electrochemical oxidation of h2o2 on pt and pt + ir electrodes in physiological buffer and its applicability to h2o2-based biosensors. *J. Electroanal. Chem.* **1993,** *345* (1), 253-271.

17. Huffman, M. L.; Venton, B. J., Carbon-fiber microelectrodes for in vivo applications. *Analyst (Cambridge, U. K.)* **2009,** *134* (1), 18-24.

18. Ross, A. E.; Venton, B. J., Nafion-cnt coated carbon-fiber microelectrodes for enhanced detection of adenosine. *Analyst* **2012,** *137* (13), 3045-3051.

19. Wynne, A.; Finnerty, N., Ascorbic acid rejection characteristics of modified platinum electrodes: A shelf life investigation. *Chemosensors* **2015,** *3* (2), 55.

20. Taylor, I. M.; Robbins, E. M.; Catt, K. A.; Cody, P. A.; Happe, C. L.; Cui, X. T., Enhanced dopamine detection sensitivity by pedot/graphene oxide coating on in vivo carbon fiber electrodes. *Biosens. Bioelectron.* **2017,** *89* (Pt 1), 400-410.

21. Ganesana, M.; Lee, S. T.; Wang, Y.; Venton, B. J., Analytical techniques in neuroscience: Recent advances in imaging, separation, and electrochemical methods. *Anal. Chem. (Washington, DC, U. S.)* **2017,** *89* (1), 314-341.

22. Yuan, B.; Xu, C.; Liu, L.; Shi, Y.; Li, S.; Zhang, R.; Zhang, D., Polyethylenimine-bridged graphene oxide–gold film on glassy carbon electrode and its electrocatalytic activity toward nitrite and hydrogen peroxide. *Sensors Actuators B: Chem.* **2014,** *198*, 55-61.

23. Ambrosi, A.; Chua, C. K.; Latiff, N. M.; Loo, A. H.; Wong, C. H.; Eng, A. Y.; Bonanni, A.; Pumera, M., Graphene and its electrochemistry - an update. *Chem. Soc. Rev.* **2016,** *45* (9), 2458-2493.

24. Bai, J.; Wu, L.; Wang, X.; Zhang, H.-M., Hemoglobin-graphene modified carbon fiber microelectrode for direct electrochemistry and electrochemical h2o2 sensing. *Electrochim. Acta* **2015,** *185*, 142-147.

25. Janegitz, B. C.; Silva, T. A.; Wong, A.; Ribovski, L.; Vicentini, F. C.; Taboada Sotomayor, M. D.; Fatibello-Filho, O., The application of graphene for in vitro and in vivo electrochemical biosensing. *Biosens. Bioelectron.* **2017,** *89* (Pt 1), 224-233.

26. Zhu, M. F.; Zeng, C. Q.; Ye, J. S., Graphene-modified carbon fiber microelectrode for the detection of dopamine in mice hippocampus tissue. *Electroanalysis* **2011,** *23* (4), 907-914.

27. Bai, J.; Wang, X.; Meng, Y.; Zhang, H. M.; Qu, L., Fabrication of graphene coated carbon fiber microelectrode for highly sensitive detection application. *Anal. Sci.* **2014,** *30* (9), 903-909.

28. Lightcap, I. V.; Kosel, T. H.; Kamat, P. V., Anchoring semiconductor and metal nanoparticles on a two-dimensional catalyst mat. Storing and shuttling electrons with reduced graphene oxide. *Nano Lett.* **2010,** *10* (2), 577-583.

29. Hashemi, P.; Dankoski, E. C.; Petrovic, J.; Keithley, R. B.; Wightman, R. M., Voltammetric detection of 5-hydroxytryptamine release in the rat brain. *Anal. Chem.* **2009,** *81* (22), 9462-9471.

30. Heien, M. L.; Johnson, M. A.; Wightman, R. M., Resolving neurotransmitters detected by fast-scan cyclic voltammetry. *Anal. Chem.* **2004,** *76* (19), 5697-5704.

31. Sanford, A. L.; Morton, S. W.; Whitehouse, K. L.; Oara, H. M.; Lugo-Morales, L. Z.; Roberts, J. G.; Sombers, L. A., Voltammetric detection of hydrogen peroxide at carbon fiber microelectrodes. *Anal. Chem.* **2010,** *82* (12), 5205-5210.

Chapter 3: H_2O_2 and post chemotherapy cognitive impairment (PCCI)

1. Introduction

1.1 Post chemotherapy cognitive impairment

Approximately 20-30% of cancer patients who have received chemotherapy treatments suffer from post chemotherapy cognitive impairment (PCCI), also known as 'chemo brain.' PCCI is a cognitive syndrome associated with a general decline in cognitive function, memory skills and attention deficits.[1, 2] Some common symptoms of PCCI include confusion, fatigue, and short attention span, difficulty learning new skills, inability to effectively multitask, and taking longer than usual to complete routine tasks.[3] Although the causes of PCCI are still not clear, recent evidence suggests that it may be caused by several mechanisms. These include genetic factors such as impaired DNA dysregulation, DNA damage, blood brain barrier (BBB) dysfunction, and dysfunction of the immune system.[4-6] In addition to these potential factors, alterations in neurotransmitter signaling may be impaired by inherent toxicity of several types of chemotherapeutic agents, thereby altering brain function.[7-10]

1.2 Chemotherapy and common chemotherapeutic agents

Chemotherapy is a type of cancer treatment in which toxic agents are used to destroy cancer cells based on their faster rate of division. Depending on the type and the severity of the cancer, chemotherapy can cure/control the cancer or ease the cancer symptoms. Often, chemotherapy is used along with surgery, radiation therapy or biological therapy. There are two types of chemotherapy treatments neo–adjuvant chemotherapy and adjuvant chemotherapy. Neo–adjuvant chemotherapy is used to shrink a tumor before surgery or radiation therapy

whereas adjuvant chemotherapy destroys cancer cells that may remain after surgery or radiation therapy. Furthermore, chemotherapy is often used to enhance the effectiveness of biological therapies in destroying recurrent cancer cells and preventing metastatic cancer (spread to other parts of your body). Chemotherapy can be given in several ways including oral, intravenous (IV) and injection. Table 1 illustrates the different ways that chemotherapy is administered.[11, 12]

Table 1. Routes of administration of chemotherapeutic drugs

Type	Description
Oral	Chemotherapeutic drug comes in a pill or tablet that the patient can swallow
Intravenous (IV)	Chemotherapeutic drug is placed directly in to a vain
Injection	Drug is given by a shot in a muscle in your arm, thigh or hip or right under the skin in the fatty part of your arm, leg or belly.
Intrathecal	Drug is injected in to the space between layers of tissue that cover the brain and the spinal cord.
Intraperitoneal (IP)	Drug goes directly in to the peritoneal cavity.
Intra-arterial	Drug is injected directly in to the artery that leads to the cancer.
Topical	Chemo drug comes in a cream that the patient can rub on to the skin.

Importantly, both dividing and non-dividing cell populations in the CNS are vulnerable to the effects of chemotherapeutic agents.[11-13] The type of chemotherapy drug, dose, and treatment schedule depend on the following factors; type of cancer, tumor size and location and the stage of the cancer, age and general health, how well the patient can cope with certain side effects, other medical conditions and previous cancer treatments. Sometimes a combination of drugs (which means you are receiving two or three drugs at the same time) are given to make the

treatment effective. There are different types of chemotherapy drugs including Cytoxan, Carboplatin, 5-fluorouracil (brand name Adrucil), Doxorubicin (Doxil).

1.3 Possible causes of PCCI

As mentioned earlier, PCCI is the chemotherapy related cognitive impairment or cognitive dysfunction. Researchers have shown that there can be multiple causes behind the cognitive dysfunction that many cancer survivors experience. Loss of the structure or the function of the neurons is called the neurodegeneration. Neurotransmitter signaling can be affected by the toxicity of the chemotherapy drugs. It has been discovered that progenitor cells and oligodendrocytes in the brain are highly sensitive to some chemotherapy drugs.[14] Hence, to provide an effective chemotherapy treatment with lesser side effects, it is essential to study the mechanism of the neurodegeneration which causes the PCCI.

Previous studies done in our group have revealed that dopamine (which is an important neurotransmitter for cognitive function) release and uptake in the striatum, evoked by electrical stimulation, is impaired as a result of chemotherapy treatment.[15] Although the reason for this decrease in release is not clear, it is possible that the terminals of the neurons may be damaged by reactive oxygen species (ROS). Hydrogen peroxide (H_2O_2), a well-known ROS that is generated in several ways, including as a by-product of mitochondrial respiration, has the potential to cause cellular damage. Additionally, H_2O_2 can act as a neuromodulator for DA.[16, 17] In this work, we evaluated two chemotherapeutic agents in rats in order to measure their effects on H_2O_2 production.

1.4 H_2O_2 as a neuromodulator

Recent findings have suggested that H_2O_2 is an inter- and intra-cellular signaling molecule as well as a local neuromodulator of the release of dopamine, a neurotransmitter that plays a crucial role in motor and cognitive function.[17, 18] One way that H_2O_2 may be generated is

by activation of glutamatergic AMPA receptor on medium spiny neurons in the striatum. This endogenously produced H_2O_2 can inhibit DA release by activating the ATP sensitive K^+_{ATP} channels.[19] These channels, which are gated by intracellular nucleosides ATP and ADP and are found in the plasma membrane and subcellular membranes, are composed of K_{ir} 6.X – type subunits and sulfonylurea receptor (SUR) subunits with other additional components.[20] K_{ATP} channel levels are particularly high in the striatum and the substantia nigra (SN) compared to other brain regions.[19, 21-23] Initial evidence that H_2O_2 could act as a neuromodulator came when it was found that exogenously applied H_2O_2 decreased the amplitude of evoked population spikes in hippocampal slices.[24, 25] Many other experiments have been performed to assess the effect of H_2O_2 on evoked DA release in striatal brain slices.

Figure 1 illustrates the activation of K_{ATP} channels by elevated H_2O_2. It is important to note that, under normal conditions, H_2O_2 levels are tightly regulated by peroxidase enzymes, such as glutathione (GSH) peroxidase and catalase,[16] both of which catalyze reduction of H_2O_2 to water. Endogenous H_2O_2 levels can be elevated by addition of inhibitors of peroxide scavenging enzymes; for example, mercaptosuccinate (MCS), which is an efficient glutathione peroxidase inhibitor, has been used for this purpose.

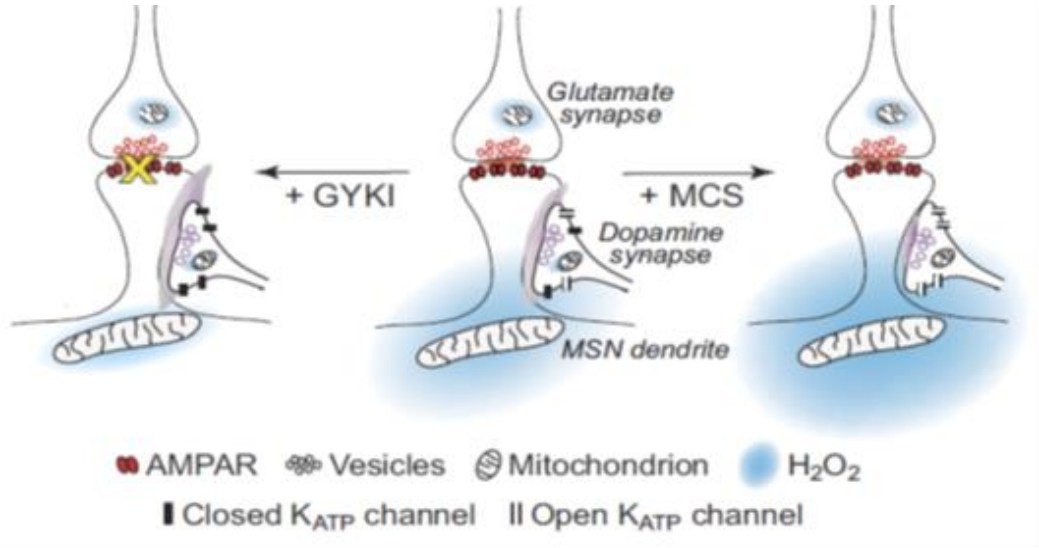

Figure 1. Schematic diagram depicting the activation of K_{ATP} channels via elevated endogenous H_2O_2 by MCS [26]

1.5 Detection of H_2O_2 with FSCV

As mentioned in the Chapter 1, background subtracted FSCV is an electrochemical technique that is well suited for measuring sub-second changes in concentrations of electroactive neurotransmitters, such as dopamine and serotonin.[27] This method provides good selectivity, high spatial resolution, and excellent temporal resolution.[28]

The detection of H_2O_2 with FSCV has recently been described by Sanford et al.[29, 30] To selectively detect H_2O_2, the waveform is ramped up to +1.4V from a holding potential -0.4V and swept back at a scan rate of 400 V/s.[16] After background subtraction, the irreversible oxidation of H_2O_2 is detected on the cathodic scan (Figure 2).

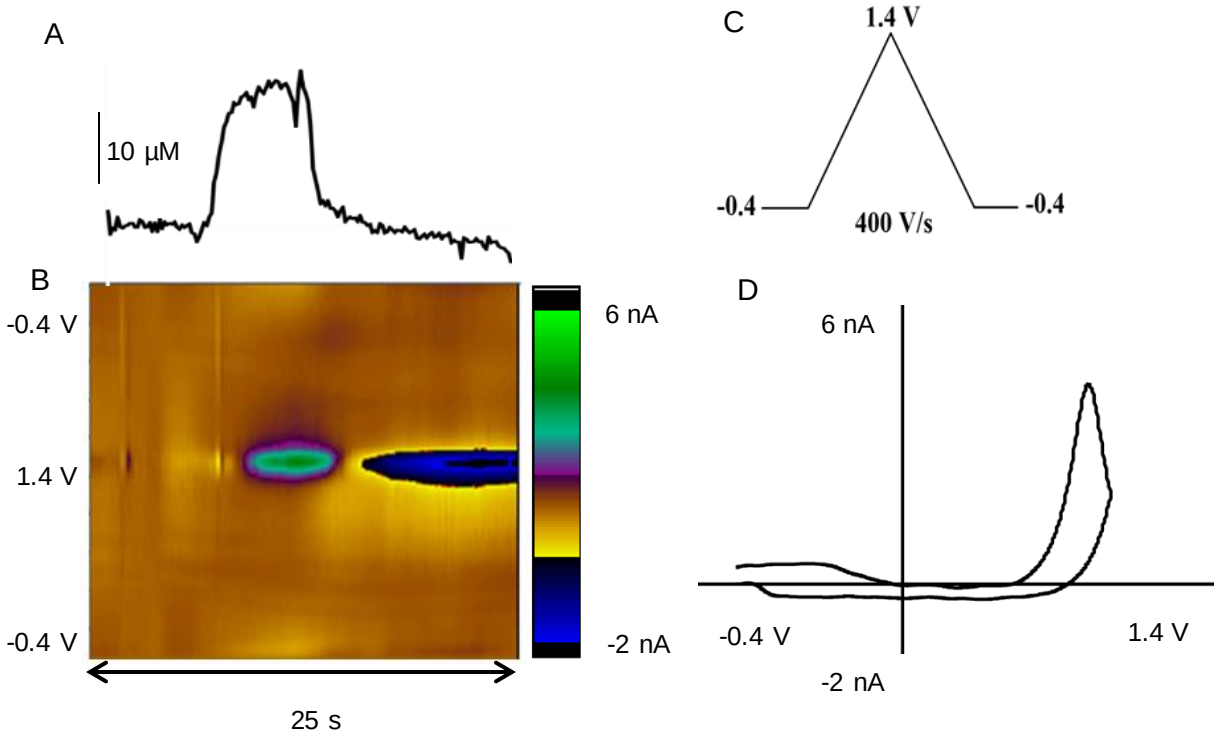

Figure 2. A current plot (A) is shown above the corresponding color plot (B). The applied wave form was -0.4V to 1.4V to -0.4V (C), and was used to generate the characteristic cyclic voltammogram (D) of H_2O_2.

Each cycle is repeated every 100 ms, offering sub-second temporal resolution. The procedures for FSCV have been described in more detail in Chapter 2. Briefly, the voltammograms are unfolded at the switching potential and stacked with respect to collection time. A color plot is generated where the Y axis represents the applied potential in V, the X axis represents the collection time in seconds and the Z axis represents the current in nA.[31] From a color plot a cyclic voltammogram and a current Vs time trace may be extracted.

1.6 Carboplatin and 5-Fluorouracil as chemotherapeutic agents

1.6.1 Carboplatin – (cis Diammine(1,1cyclobutanedicarboxylato)platinum (II))

Structure of Carboplatin is shown in Figure 3. It is a common chemotherapeutic drug used to treat various cancer types mainly ovarian, lung, neck and head. Carboplatin was introduced in 1980, after the accidental discovery of anticancer properties of cisplatin, which was a major landmark in the history of developing effective chemotherapy drugs.[32, 33]

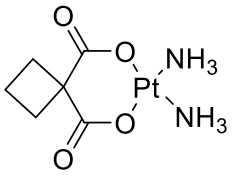

Figure 3. Structure of carboplatin

Similar to cisplatin, carboplatin belongs to the platinum based antineoplastic agents and interfere with DNA repair by interacting with DNA. The mechanism of carboplatin is similar to that of cisplatin in that it forms interstrand and intrastrand DNA crosslinks which leads to cell growth inhibition and apoptosis.[34-36] However, carboplatin has less server side effects compared to cisplatin.[37] Carboplatin is typically given to the patients by intravenous (IV) injections.[38]

1.6.2 5- Fluorouracil

Since, 1957, 5- Fluorouracil (5-FU) has been widely used as a chemotherapy drug. It has been used to treat colon cancer, breast cancer and other types of cancers, like neck and head. 5-FU is given intravenously (IV). It is a heterocyclic aromatic compound and its structure is similar to the structure of pyrimidine molecule of DNA and RNA. It is categorized as an antimetabolite which are very similar to the substances in the cell. Furthermore, it is classified as an analogue of uracil.[39] In 5-FU, a fluorine atom is at the C-5 position in place of the hydrogen atom. Hence, 5-FU can incorporated in to DNA and RNA and interfere with nucleoside metabolism. This leads to cytotoxicity and cell death. Figure 4 shows the chemical structures of 5-FU and Uracil. Another anticancer effect of 5-FU arises from its inhibition of thymidylate

synthase (TS), an enzyme that catalyzes the biosynthesis of thymidylate.[40, 41] Thymidilate is necessary for DNA replication and repair. Hence it absence causes the cell death.

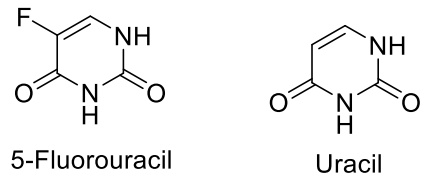

Figure 4. Chemical structures of 5-fluorouracil and uracil[42]

1.7 KU-32 as a neuroprotective agent

KU-32, developed by Dr. Brian Blagg at KU (Figure 6), is a novel novobiocin-based C-terminal inhibitor of Hsp90 and increases the expression of Hsp70 and thereby induces a protective cellular heat shock response. As a neuroprotective agent, it has been found that KU-32 is capable of preventing and reversing the diabetic peripheral neuropathy (DPN) in mice[43] as well as protect against glucose-induced death of embryonic DRG (dorsal root ganglia) neurons.[43] DPN is usually associated with demyelination, axonal atrophy, blunted regenerative potential and loss of peripheral nerve fibers.[44] Moreover, Hsp90 inhibitors are being used as chemotherapeutic and neuroprotective agents. Its mean half-life ($t_{1/2}$) is found to be 105.6 minutes in plasma and 106.9 minutes in brain tissue.[45]

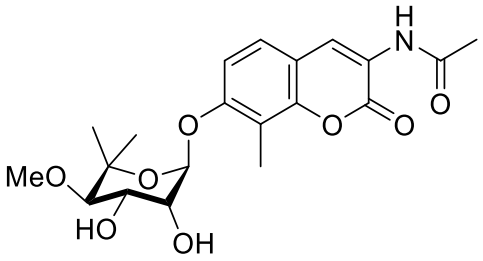

Figure 5. The chemical structure of KU-32 [44]

1.8 Organization of this Chapter. The Experimental Procedures and Results and Discussion sections of this chapter are each divided into three sections: (1) Measuring H_2O_2 levels in carboplatin treated rats, (2) Probing H_2O_2 levels in 5-FU treated rats, (3) Treatment of 5-FU-treated rats with KU-32. This organization is the most logical, given that experiments with multiple batches of rats were accomplished. Thus, each section is indicative of the goal for each particular experiment.

2. Experimental Procedures

2.1 Experimental Procedures: (1) Measuring H_2O_2 levels in carboplatin treated rats

2.1.1 Animals

All experiments were carried out in accordance with the National Institute of Health guide for the care and use of laboratory animals. All the procedures were approved by the University of Kansas institutional Animal Care and use Committee. Experiments were carried out using male Wistar rats (Charles River Laboratories, Inc., Wilmington, MA, USA). Rats were housed 3 per cage in the University of Kansas Institutional Animal Care Unit. Food and water were supplied at libitum. Rats were maintained on a 12 hour light / dark cycle with lights on at 6.00 AM and lights out at 6.00 PM. A temperature of 70 ± 2 °C and a humidity level of 50 ± 20% was maintained.

2.1.2 Carboplatin treatment

Carboplatin (lot number 61703-339-50) was purchased from Hospira (Lake Forest, IL, USA). ~~And~~ Mercaptosuccinic acid was purchased from sigma Aldrich. Male wistar rats received one injection (IV, Tail vein) of carboplatin (30 mg/Kg) once a week for four consecutive weeks. All the drug solutions were made in biological saline. Both dosage and treatment regimens have been chosen to mimic a reasonable clinical dosing regimens and to allow for the drug effect to stabilize.

2.1.3 Carbon fiber Micro Electrode fabrication

Electrode fabrication was discussed in more detail in Chapter 2. Briefly, carbon-fiber microelectrodes were made in-house. Carbon-fibers, 7 µm in diameter, were loaded into glass capillaries (4 in, 1.2mm OD; A-M System, Inc. Carlsberg, WA, USA) and pulled using an electrode puller (Narishige International USA, East Meadow, NY, USA). Carbon-fiber tips were cut using a scalpel 50 µm from the end of the glass seal. Then the electrodes were sealed using an epoxy mixture of 0.24 grams EPI-CURE 3234 Curing Agent and 2.00 grams EPON Resin 815C. Excess resins removed by dipping the electrodes several times in toluene. Finally, the electrodes were baked for 1 hour at 100 °C. The electrodes were back filled with 0.5 M potassium acetate in order to establish an electrical connection.

2.1.4 Brain slice preparation

Rats were anesthetized by isoflurane inhalation and decapitated by Rachel Ginther. Then the brain was immediately removed and placed in ice-cold artificial cerebral spinal fluid (aCSF). The aCSF solution consist of (in mM) 126 NaCl, 2.5 KCl, 25 $NaHCO_3$, 1.2 NaH_2PO_4, 2.4 $CaCl_2$, 1.2 $MgCl_2$, 20 HEPES, 11 D- glucose. PH was adjusted to 7.4. aCSF solution was continuously saturated with 95% O_2 / 5% CO_2 throughout the experiment to ensure the tissue receives ample oxygen.

The cerebellum was sliced with a sterilized razor blade. One hemisphere of the brain was flash frozen on dry ice and was stored at - 80 °C while the other hemisphere was mounted to a agar block using glue. 300 µm thick coronal brain slices were prepared using an NVSL vibratome (Leica Microsystems, Bannockburn, IL, USA). In one recording session, a single striatal brain slice was transferred to a perfusion chamber and submerged in oxygenated aCSF continuously flowing (2 mL/min) maintained at 34 °C using a thermostatted perfusion chamber and in-line

heater. Brain slice was allowed to equilibrate for 1 hour after transferring to the perfusion chamber. Then the measurements were collected.

2.1.5 Electrochemical Measurements Using FSCV

In a typical brain slice experiment, pre calibrated cylinder carbon-fiber microelectrodes were inserted using micromanipulators and a stereoscope until the tip was 100 µm below the surface of the brain slice. A diagram of the experimental setup is shown in Figure 6. The carbon-fiber working electrode was positioned between two biphasic stimulating electrodes in the striatum. A triangular waveform, starting at -0.4 V ramping up to 1.4 V and back to -0.4 V was applied to the working electrode at a scan rate of 400 V/s and an update rate of 10 Hz. An Ag/AgCl reference electrode was used. Dopamine (DA) release was evoked by applying a single biphasic pulse (350 µA, 4 ms total duration) to the stimulating electrode. First, a baseline DA signal was established to ensure slice viability in the striatum. A 5 minutes recovery period was allowed between each measurement. DA oxidation current was measured and plotted versus potential and the successive voltammograms were plotted against time. Same wave form was applied to measure H_2O_2. For quantification of H_2O_2 release, a baseline DA was determined to ensure the slice viability. After establishing the DA signal, 1 mM MCS (mercaptosuccinic acid) was introduced to the slice to elevate endogenous H_2O_2 levels. After introducing the MCS a long file was collected for 130 seconds. Subsequent files (20 seconds) were collected to determine the H_2O_2 levels. In each color plot the back ground was subtracted to the minimum current. At the end of each recording session, catalase (10µM) was introduced to the brain slice to confirm the disappearance of the electrochemical currents, confirming the presence of H_2O_2. This procedure was followed for all the files in which MCS was used. The concentration of H_2O_2 released was determined by calibration of electrodes. The calibration factors were obtained by averaging values from pre- and post-calibrations.

2.1.6 Statistics

Statistical analyses were performed using graph pad prism software (Graph pad software Inc., San Diego, CA, USA). n =5 number of rats. Student t test was performed ($p<0.05$)

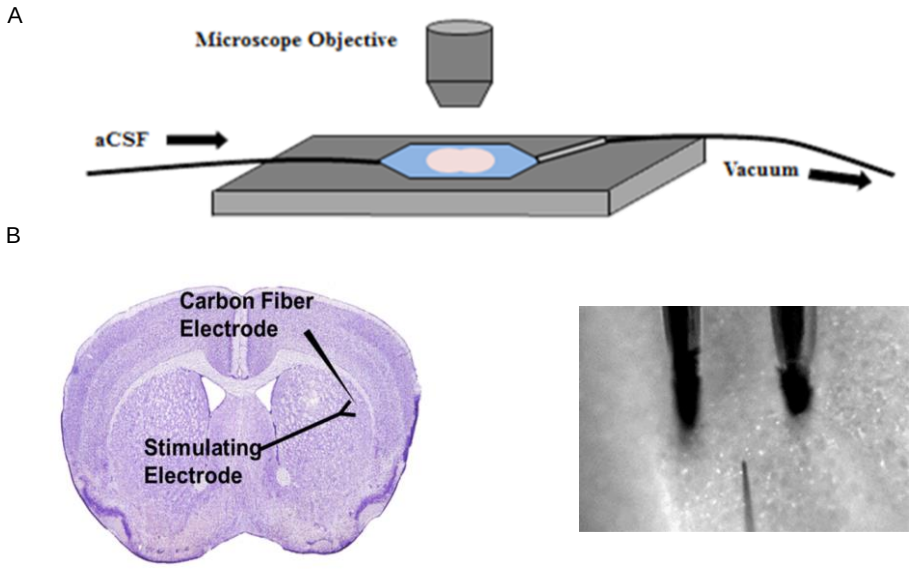

Figure 6. The experimental set up of a brain slice experiment. (A) Brain slice is placed in the perfusion chamber and a continuous acsf buffer flow is supplied. (B) Stimulating electrode and working electrode is placed in to the striatum

2.2 Experimental Procedures: (2) Measuring H_2O_2 levels in 5-FU treated rats

2.2.1 Animals

All experiments were carried out using male Wistar rats (Charles River Laboratories, Inc., Wilmington, MA, USA). Rats were housed 3 per cage in the University of Kansas Institutional Animal Care Unit. Food and water were supplied at libitum. Rats were maintained on a 12 hour light / dark cycle with lights on at 6.00 AM and lights out at 6.00 PM. A temperature of 70 ± 2 °C and a humidity level of 50 ± 20% were maintained**.**

2.2.2 Drugs

Pharmaceutical grade 5-Fluorouracil was purchased from Sigma Aldrich

2.2.3 Drug treatment

Male wistar rats received one injection (IV, Tail vein) of 5-FU (25mg/Kg) once a week for two consecutive weeks. All the drug solutions were made in biological saline. Both dosage and treatment regimens have been chosen to mimic a reasonable clinical dosing regimen and to allow for the drug effect to stabilize.

2.2.4 Brain slice preparation

H_2O_2 probing was performed a week after the treatments.Brain slice preparation and FSCV measurements were done as mentioned before.

2.2.5 H_2O_2 quantification

H_2O_2 levels were quantified in each rat group in a similar way to the carboplatin experiment.

2.2.6 Statistics

ANOVA with Post HOC test was used to determine statistical differences. $P<0.05$. GraphPad prism 5 (Graphpad Software, Inc, La Jolla, CA) was used for graphical and statistical analysis.

2.3 Experimental Procedures: (3) Treatment of 5-FU-treated rats with KU-32

2.3.1 Animals

All experiments were carried out using male Wistar rats (Charles River Laboratories, Inc., Wilmington, MA, USA). Rats were housed 3 per cage in the University of Kansas Institutional Animal Care Unit. Food and water were supplied at libitum. Rats were maintained

on a 12 hour light / dark cycle with lights on at 6.00 AM and lights out at 6.00 PM. A temperature of 70 ± 2 °C and a humidity level of 50 ± 20% were maintained.

2.3.2 Drugs

All chemotherapeutic agents were purchased from Sigma Aldrich and KU32 was supplied by Dr. Blagg research group at Department of Medicinal Chemistry at the University of Kansas.

2.3.3 Drug treatment

Male wistar rats received one injection (IV, Tail vein) of 5FU (30 mg/Kg) and (20mg/Kg) once a week for four consecutive weeks. For the combination treatment, rats were administered 5FU (20 mg/Kg) IV, Tail vein. On the same day KU32 was administered via oral gavage route (20 mL/Kg). All the drug solutions were made in biological saline. Both dosage and treatment regimens have been chosen to mimic reasonable clinical dosing regimens and to allow for the drug effect to stabilize**.**

2.3.4 Brain slice preparation

H_2O_2 probing was performed 2 weeks after the treatments. Brain slice preparation and FSCV measurements were done as mentioned before.

2.3.5 H_2O_2 quantification

H_2O_2 levels were quantified in each rat group in a similar way to the carboplatin experiment.

2.3.6 Statistics

2 way ANOVA was used to determine statistical differences. $P< 0.05$. GraphPad prism 5 (Graphpad Software, Inc, La Jolla, CA) was used for graphical and statistical analysis.

All the chemotherapy treatments were carried out by Rachel Ginther.

3. Results and Discussion

3.1 (1) Measuring H_2O_2 levels in carboplatin treated rats

A representative file for H_2O_2 measurement after MCS treatment is shown in Figure 7. Each peak was recorded and averaged across all of the files to determine the overall H_2O_2 levels. As the release is spontaneous, several sample analyses showed multiple peaks corresponding to release events. H_2O_2 levels were elevated upon the addition of 1 mM MCS. As was mentioned,

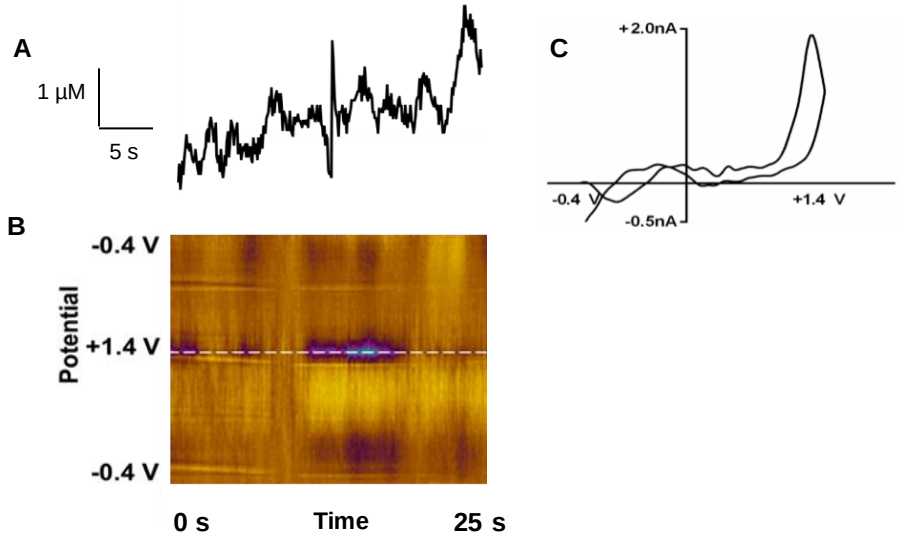

Figure 7. Schematic diagram which shows spontaneous release of H_2O_2 in rat striatal brain slice after inhibition of glutathione peroxidase with MCS. (A) Current plot (B) Representative color plot. (C) cyclic voltammogram of H_2O_2.

MCS is an efficient inhibitor of glutathione peroxidase, an antioxidant enzyme that catalyzes the decomposition of H_2O_2 to water. Addition of MCS prevents this decomposition, thereby

enhancing endogenous H_2O_2 levels.[17, 18] Detected peroxide levels were greater in carboplatin treated rats compared to the saline treated rats as shown in Figure 8 (t-test $p < 0.05$, $n = 5$). Hence, these data indicated a high free radical activity in chemotherapy treated rats.

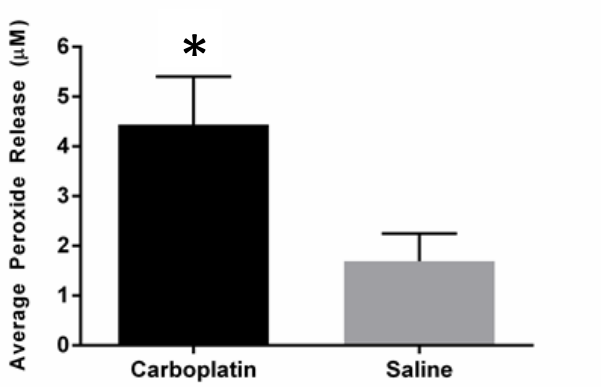

Figure 8. H_2O_2 levels are greater in carboplatin treated rats compared to vehicle treated rats. *P<0.05 (t-test, carboplatin n = 5, vehicle n = 5).

These results suggests that carboplatin treatment results in an increase of H_2O_2 levels that persists at least one week after the last injection (rats underwent neurochemical analysis at this time). This enhanced production could have several long-term consequences. Given that H_2O_2 is a reactive oxygen species, neuronal dysfunction could result directly from chemical oxidative damage. Additionally, H_2O_2 has been shown to elicit an immune response, thereby activating biochemical pathways that result in the production of inflammatory cytokines, such as tumor necrosis factor alpha (TNFα).[46] Elevated TNFα levels, induced by ROS production, have already been implicated in post-chemotherapy cognitive impairment (PCCI) associated with doxorubin chemotherapy,[46] which is often used to treat breast cancer.[46, 47] Also H_2O_2 is a neuromodulator in the DA pathway. This increased endogenous H_2O_2 levels can affect DA release and uptake causing cognitive dysfunction.[48] Finally, as alluded to earlier in this chapter, H_2O_2 serves a role as a neuromodulator and may cause chronically diminished dopamine release.

3.2 (2) Measuring H_2O_2 levels in 5FU treated rats

A representative file for H_2O_2 release following 5FU treatment is shown in Figure 9. An increased oxidation current was observed for the H_2O_2 in 5FU treated rats compared to the vehicle treated. The detected peroxide levels were 151% greater in 5FU treated group than the vehicle treated group (5FU n = 5, Vehicle n = 3, ANOVA $p<0.05$)(Figure 10). Upon the introduction of MCS the current generated was enhanced. Disappearance of oxidation current after the introduction of 1 U/ml catalase verified that the observed current was due to the oxidation of H_2O_2 (Figure 11). These data suggest that free radical activity is greater in 5FU treated rats.

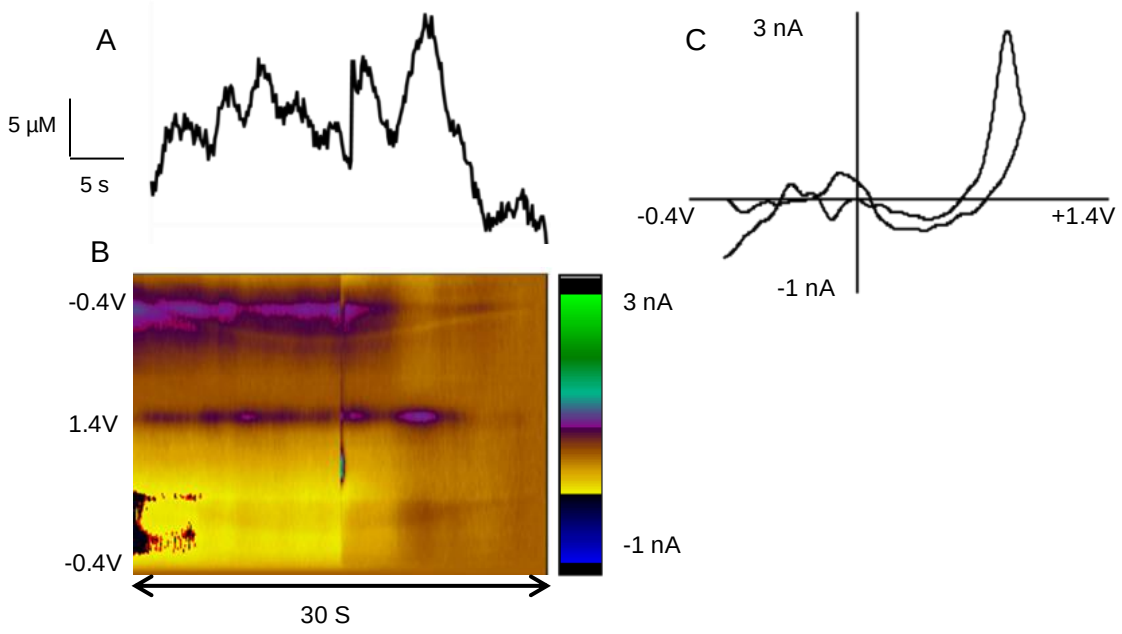

Figure 9. Spontaneous release of H_2O_2 in rat striatal brain slice after inhibition of glutathione peroxidase with MCS; (A) Current Plot, (B) Representative color plot, and (C) cyclic voltammogramm for H_2O_2.

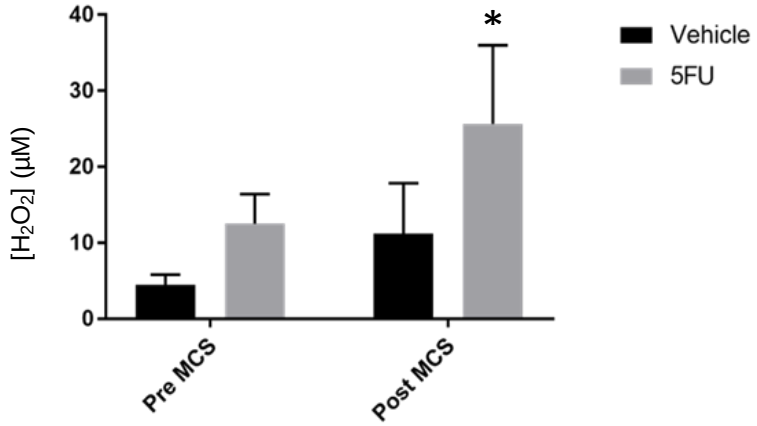

Figure 10.Enhanced levels of H_2O_2 in brain slices from 5-FU treated rats. *P< 0.05 (ANOVA with post hoc test, treated n=5, vehicle n=3).

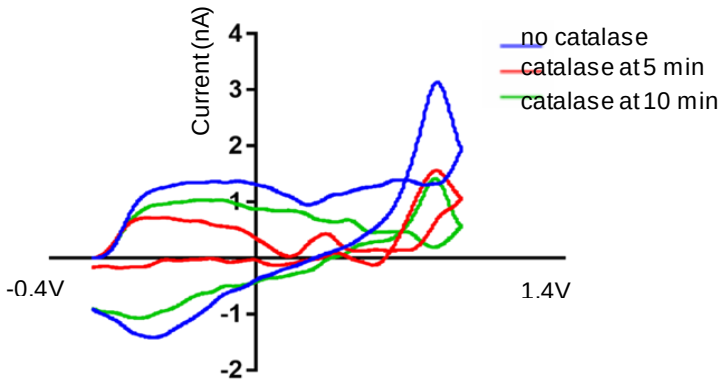

Figure 11. Cyclic voltammograms obtained before introducing catalase and after introducing catalase (Enzymatic degradation of H_2O_2). Oxidation current for H_2O_2 decreased upon addition of 1U/ml catalase Fig (12). About 15 minutes after the introduction of catalase, the oxidation current obtained for H_2O_2 was further diminished, suggesting that the current was due to oxidation of H_2O_2.

3.3 (3) Treatment of 5FU-treated rats with KU-32

To determine the effect of KU-32 on the spontaneous release of H_2O_2, three treatment groups (Saline , 5FU, 5FU+KU32) were compared. Results from multiple rats are shown in Figure 12. H_2O_2 levels in 5FU treated rats were significantly increased compared to vehicle treated and 5FU+KU32 treated rats (n=5, 5FU+KU32 n=3, vehicle n=5, Two way ANOVA with post hoc test, $P < 0.05$). These results suggest that treatment with 5-FU results in enhanced levels of H_2O_2 and that KU-32 brings levels back to normal. However, it is not yet clear whether 5-FU decreases the production of H_2O_2 or diminishes the antioxidant capacity of the brain. On the other hand, KU-32 is known to induce the heat shock response and upregulate proteins that are protective to cells. These proteins likely include those which serve an antioxidant role. Nevertheless, additional work will be required to determine specifically which proteins are upregulated and to what extent in the 5-FU chemo brain model.

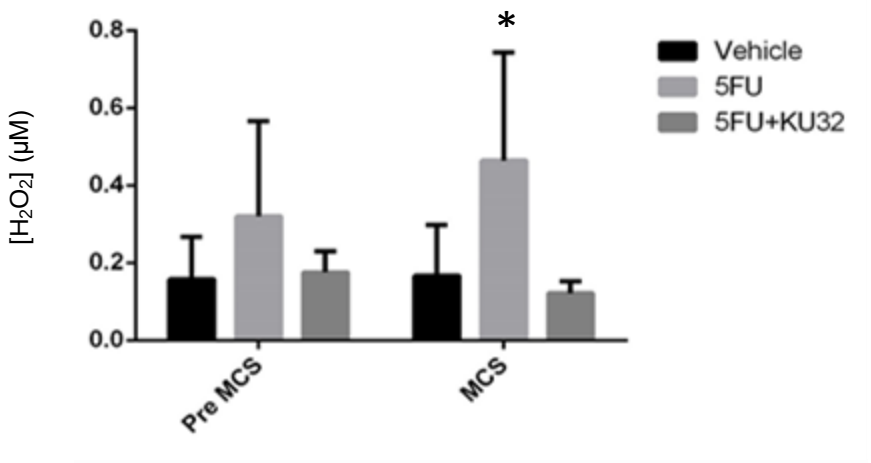

Figure 12. KU-32 restored H_2O_2 levels to normal in 5FU treated rats. *$P < 0.05$ (two-way ANOVA, 5FU treated n=5, 5FU+KU32 n=3, vehicle n=5).

4. Conclusions

These data revealed that peroxide levels are greater in chemotherapy treated rats compared to the vehicle treated rats. As discussed, H_2O_2 may have a number of deleterious effects on neuronal function including oxidative damage, inflammation, and neuromodulation. Because dopamine's multiple roles as a neurotransmitter, reward,[49] cognition,[50] locomotion, and behavior[50, 51] may all be affected. Studies done in our group have revealed that DA uptake and release is impaired in chemotherapy treated rats,[15] suggesting that increased H_2O_2 levels are a contributing factor in post chemotherapy cognitive impairment. Furthermore, combination of 5-FU with KU-32 which is a neuroprotective agent has suppressed the elevated H_2O_2 levels, reversing the neuronal degeneration and replacing the proper function of neurons. KU 32 is an inhibitor of Hsp90 heat shock protein which can increase the expression of Hsp70. Researchers think that enhancement in Hsp70 expression may inhibit neuronal degeneration and improve the proper function of neurons.[52]

References

1. Nelson, C. J.; Nandy, N.; Roth, A. J., Chemotherapy and cognitive deficits: Mechanisms, findings, and potential interventions. *Palliative & supportive care* **2007,** *5* (3), 273-280.

2. Boykoff, N.; Moieni, M.; Subramanian, S. K., Confronting chemobrain: An in-depth look at survivors' reports of impact on work, social networks, and health care response. *J. Cancer Surviv.* **2009,** *3* (4), 223-232.

3. Weiss, B., Chemobrain: A translational challenge for neurotoxicology. *Neurotoxicology* **2008,** *29* (5), 891-898.

4. Ahles, T. A.; Saykin, A. J., Candidate mechanisms for chemotherapy-induced cognitive changes. *Nat. Rev. Cancer* **2007,** *7* (3), 192-201.

5. Hoffmeyer, S.; Burk, O.; von Richter, O.; Arnold, H. P.; Brockmoller, J.; Johne, A.; Cascorbi, I.; Gerloff, T.; Roots, I.; Eichelbaum, M.; Brinkmann, U., Functional polymorphisms of the human multidrug-resistance gene: Multiple sequence variations and correlation of one allele with p-glycoprotein expression and activity in vivo. *Proc. Natl. Acad. Sci. U. S. A.* **2000,** *97* (7), 3473-3478.

6. von Zglinicki, T., Oxidative stress shortens telomeres. *Trends Biochem. Sci* **2002,** *27* (7), 339-344.

7. de Visser, K. E.; Eichten, A.; Coussens, L. M., Paradoxical roles of the immune system during cancer development. *Nat. Rev. Cancer* **2006,** *6* (1), 24-37.

8. Scheibel, R. S.; Valentine, A. D.; O'Brien, S.; Meyers, C. A., Cognitive dysfunction and depression during treatment with interferon-alpha and chemotherapy. *J. Neuropsychiatry Clin. Neurosci.* **2004,** *16* (2), 185-191.

9. Kelley, K. W.; Bluthe, R. M.; Dantzer, R.; Zhou, J. H.; Shen, W. H.; Johnson, R. W.; Broussard, S. R., Cytokine-induced sickness behavior. *Brain. Behav. Immun.* **2003,** *17 Suppl 1*, S112-118.

10. Meyers, C. A.; Albitar, M.; Estey, E., Cognitive impairment, fatigue, and cytokine levels in patients with acute myelogenous leukemia or myelodysplastic syndrome. *Cancer* **2005,** *104* (4), 788-793.

11. Sawyer, A. J.; Piepmeier, J. M.; Saltzman, W. M., New methods for direct delivery of chemotherapy for treating brain tumors. *Yale J. Biol. Med.* **2006,** *79* (3-4), 141-152.

12. Ferguson, S.; Lesniak, M. S., Convection enhanced drug delivery of novel therapeutic agents to malignant brain tumors. *Curr Drug Deliv* **2007,** *4* (2), 169-180.

13. Ciordia, R.; Supko, J.; Gatineau, M.; Batchelor, T., Cytotoxic chemotherapy: Advances in delivery, pharmacology, and testing. *Curr. Oncol. Rep.* **2000,** *2* (5), 445-453.

14. Dietrich, J.; Han, R.; Yang, Y.; Mayer-Proschel, M.; Noble, M., Cns progenitor cells and oligodendrocytes are targets of chemotherapeutic agents in vitro and in vivo. *J. Biol.* **2006,** *5* (7), 22.

15. Kaplan, S. V.; Limbocker, R. A.; Gehringer, R. C.; Divis, J. L.; Osterhaus, G. L.; Newby, M. D.; Sofis, M. J.; Jarmolowicz, D. P.; Newman, B. D.; Mathews, T. A.; Johnson, M. A., Impaired brain dopamine and serotonin release and uptake in wistar rats following treatment with carboplatin. *ACS Chem. Neurosci.* **2016,** *7* (6), 689-699.

16. Spanos, M.; Gras-Najjar, J.; Letchworth, J. M.; Sanford, A. L.; Toups, J. V.; Sombers, L. A., Quantitation of hydrogen peroxide fluctuations and their modulation of dopamine dynamics in the rat dorsal striatum using fast-scan cyclic voltammetry. *ACS Chem. Neurosci.* **2013,** *4* (5), 782-789.

17. Rice, M. E., H2o2: A dynamic neuromodulator. *Neuroscientist* **2011,** *17* (4), 389-406.

18. Patel, J. C.; Rice, M. E., Classification of h(2)o(2)as a neuromodulator that regulates striatal dopamine release on a subsecond time scale. *ACS Chem. Neurosci.* **2012,** *3* (12), 991-1001.

19. Avshalumov, M. V.; Chen, B. T.; Koos, T.; Tepper, J. M.; Rice, M. E., Endogenous hydrogen peroxide regulates the excitability of midbrain dopamine neurons via atp-sensitive potassium channels. *J. Neurosci.* **2005,** *25* (17), 4222-4231.

20. Stephan, D.; Winkler, M.; Kuhner, P.; Russ, U.; Quast, U., Selectivity of repaglinide and glibenclamide for the pancreatic over the cardiovascular k(atp) channels. *Diabetologia* **2006,** *49* (9), 2039-2048.

21. Xia, Y.; Haddad, G. G., Major differences in cns sulfonylurea receptor distribution between the rat (newborn, adult) and turtle. *J. Comp. Neurol.* **1991,** *314* (2), 278-289.

22. Zini, S.; Tremblay, E.; Pollard, H.; Moreau, J.; Ben-Ari, Y., Regional distribution of sulfonylurea receptors in the brain of rodent and primate. *Neuroscience* **1993,** *55* (4), 1085-1091.

23. Mourre, C.; Ben Ari, Y.; Bernardi, H.; Fosset, M.; Lazdunski, M., Antidiabetic sulfonylureas: Localization of binding sites in the brain and effects on the hyperpolarization induced by anoxia in hippocampal slices. *Brain Res.* **1989,** *486* (1), 159-164.

24. Pellmar, T. C., Peroxide alters neuronal excitability in the ca1 region of guinea-pig hippocampus in vitro. *Neuroscience* **1987,** *23* (2), 447-456.

25. Pellmar, T., Electrophysiological correlates of peroxide damage in guinea pig hippocampus in vitro. *Brain Res.* **1986,** *364* (2), 377-381.

26. Avshalumov, M. V.; Patel, J. C.; Rice, M. E., Ampa receptor-dependent h2o2 generation in striatal medium spiny neurons but not dopamine axons: One source of a retrograde signal that can inhibit dopamine release. *J. Neurophysiol.* **2008,** *100* (3), 1590-1601.

27. Uttara, B.; Singh, A. V.; Zamboni, P.; Mahajan, R. T., Oxidative stress and neurodegenerative diseases: A review of upstream and downstream antioxidant therapeutic options. *Curr. Neuropharmacol.* **2009,** *7* (1), 65-74.

28. Robinson, D. L.; Venton, B. J.; Heien, M. L.; Wightman, R. M., Detecting subsecond dopamine release with fast-scan cyclic voltammetry in vivo. *Clin. Chem.* **2003,** *49* (10), 1763-1773.

29. Sanford, A. L.; Morton, S. W.; Whitehouse, K. L.; Oara, H. M.; Lugo-Morales, L. Z.; Roberts, J. G.; Sombers, L. A., Voltammetric detection of hydrogen peroxide at carbon fiber microelectrodes. *Anal. Chem.* **2010,** *82* (12), 5205-5210.

30. Roberts, J. G.; Hamilton, K. L.; Sombers, L. A., Comparison of electrode materials for the detection of rapid hydrogen peroxide fluctuations using background-subtracted fast scan cyclic voltammetry. *Analyst* **2011,** *136* (17), 3550-3556.

31. Michael, D.; Travis, E. R.; Wightman, R. M., Color images for fast-scan cv measurements in biological systems. *Anal. Chem.* **1998,** *70* (17), 586a-592a.

32. Wheate, N. J.; Walker, S.; Craig, G. E.; Oun, R., The status of platinum anticancer drugs in the clinic and in clinical trials. *Dalton transactions (Cambridge, England : 2003)* **2010,** *39* (35), 8113-8127.

33. Apps, M. G.; Choi, E. H.; Wheate, N. J., The state-of-play and future of platinum drugs. *Endocr. Relat. Cancer* **2015,** *22* (4), R219-233.

34. Hah, S. S.; Stivers, K. M.; de White, R. W.; Henderson, P. T., Kinetics of carboplatin-DNA binding in genomic DNA and bladder cancer cells as detd. By accelerator mass spectrometry. *Chem. Res. Toxicol.* **2006,** *19* (5), 622-626.

35. McWhinney, S. R.; Goldberg, R. M.; McLeod, H. L., Platinum neurotoxicity pharmacogenetics. *Mol. Cancer Ther.* **2009,** *8* (1), 10-16.

36. Wang, X., Fresh platinum complexes with promising antitumor activity. *Anti-Cancer Agents Med. Chem.* **2010,** *10* (5), 396-411.

37. Aggarwal, S. K., A histochemical approach to the mechanism of action of cisplatin and its analogues. *J. Histochem. Cytochem.* **1993,** *41* (7), 1053-1073.

38. Calvert, A. H.; Newell, D. R.; Gumbrell, L. A.; O'Reilly, S.; Burnell, M.; Boxall, F. E.; Siddik, Z. H.; Judson, I. R.; Gore, M. E.; Wiltshaw, E., Carboplatin dosage: Prospective evaluation of a simple formula based on renal function. *J. Clin. Oncol.* **1989,** *7* (11), 1748-1756.

39. Longley, D. B.; Harkin, D. P.; Johnston, P. G., 5-fluorouracil: Mechanisms of action and clinical strategies. *Nat. Rev. Cancer* **2003,** *3* (5), 330-338.

40. Miura, K.; Kinouchi, M.; Ishida, K.; Fujibuchi, W.; Naitoh, T.; Ogawa, H.; Ando, T.; Yazaki, N.; Watanabe, K.; Haneda, S.; Shibata, C.; Sasaki, I., 5-fu metabolism in cancer and orally-administrable 5-fu drugs. *Cancers (Basel)* **2010,** *2* (3), 1717-1730.

41. Noordhuis, P.; Holwerda, U.; Van der Wilt, C. L.; Van Groeningen, C. J.; Smid, K.; Meijer, S.; Pinedo, H. M.; Peters, G. J., 5-fluorouracil incorporation into rna and DNA in relation to thymidylate synthase inhibition of human colorectal cancers. *Ann. Oncol.* **2004,** *15* (7), 1025-1032.

42. Zhang, N.; Yin, Y.; Xu, S. J.; Chen, W. S., 5-fluorouracil: Mechanisms of resistance and reversal strategies. *Molecules* **2008,** *13* (8), 1551-1569.

43. Farmer, K.; Williams, S. J.; Novikova, L.; Ramachandran, K.; Rawal, S.; Blagg, B. S.; Dobrowsky, R.; Stehno-Bittel, L., Ku-32, a novel drug for diabetic neuropathy, is safe for human islets and improves in vitro insulin secretion and viability. *Exp. Diabetes Res.* **2012,** *2012*, 671673.

44. Ma, J.; Farmer, K. L.; Pan, P.; Urban, M. J.; Zhao, H.; Blagg, B. S. J.; Dobrowsky, R. T., Heat shock protein 70 is necessary to improve mitochondrial bioenergetics and reverse diabetic sensory neuropathy following ku-32 therapy. *J. Pharmacol. Exp. Ther.* **2014,** *348* (2), 281-292, 212 pp.

45. Luo, W.; Sun, W.; Taldone, T.; Rodina, A.; Chiosis, G., Heat shock protein 90 in neurodegenerative diseases. *Mol. Neurodegener.* **2010,** *5*, 24.

46. Chen, Y.; Jungsuwadee, P.; Vore, M.; Butterfield, D. A.; St Clair, D. K., Collateral damage in cancer chemotherapy: Oxidative stress in nontargeted tissues. *Mol. Interv.* **2007,** *7* (3), 147-156.

47. Walker, C. H.; Drew, B. A.; Antoon, J. W.; Kalueff, A. V.; Beckman, B. S., Neurocognitive effects of chemotherapy and endocrine therapies in the treatment of breast cancer: Recent perspectives. *Cancer Invest.* **2012,** *30* (2), 135-148.

48. Wefel, J. S.; Lenzi, R.; Theriault, R.; Buzdar, A. U.; Cruickshank, S.; Meyers, C. A., 'Chemobrain' in breast carcinoma?: A prologue. *Cancer* **2004,** *101* (3), 466-475.

49. Schultz, W., Getting formal with dopamine and reward. *Neuron* **2002,** *36* (2), 241-263.

50. Backman, L.; Nyberg, L.; Lindenberger, U.; Li, S. C.; Farde, L., The correlative triad among aging, dopamine, and cognition: Current status and future prospects. *Neurosci. Biobehav. Rev.* **2006,** *30* (6), 791-807.

51. Backman, L.; Lindenberger, U.; Li, S. C.; Nyberg, L., Linking cognitive aging to alterations in dopamine neurotransmitter functioning: Recent data and future avenues. *Neurosci. Biobehav. Rev.* **2010,** *34* (5), 670-677.

52. Urban, M. J.; Li, C.; Yu, C.; Lu, Y.; Krise, J. M.; McIntosh, M. P.; Rajewski, R. A.; Blagg, B. S.; Dobrowsky, R. T., Inhibiting heat-shock protein 90 reverses sensory hypoalgesia in diabetic mice. *ASN Neuro* **2010,** *2* (4), e00040.

CHAPTER 4

Conclusions and future directions

1.1 Novel GO/Nafion CFME Conclusions

Our novel modified carbon fiber microelectrode exhibited 5.3-fold enhancement in oxidation current of H_2O_2. Surface characterization done with Scanning Electron Microscopy and Energy Dispersive X- ray Spectroscopy confirmed the thin surface coating of GO and Nafion on the carbon fiber . Electrochemical behavior of the modified electrode was very similar to that of bare carbon fiber micro electrode. Limit of detection (LOD) for the GO/Nafion CFME was found to be 0.05 µM. Detection limit for the bare carbon fiber micro electrode is found to be 2 µM by Sanford and coworkers.[1] It revealed an enhancement in the sensitivity compared to the bare CFME. Moreover, a modified electrode was successfully used in brain slice experiments to probe H_2O_2 levels. A modified electrode was used to record the oxidation of H_2O_2 in brain slices. It demonstrated a similar electrochemical behavior compared to the bare carbon fiber micro electrode. This work shows that unique characteristics of graphene oxide make it a promising material for microelectrode modifications. In the future, this modified sensor can be used to detect other electroactive species as well. Moreover, in addition to Nafion, other electroactive polymers can be used for the modification to selectively detect other electro active species. However, one drawback is that the stability and the selectivity of the modified electrode depend on the integrity of the coating.

1.2 PCCI conclusions and future directions.

Previous studies done in our group have revealed that DA release and uptake attenuated in chemotherapy treated rats. Our hypothesis was that enhanced free radical activity due to the mitochondrial dysfunction can cause neuronal degeneration causing PCCI. Hydrogen peroxide is an important membrane permeable ROS which plays an important role in the

dopaminergic pathway. Interestingly, our data revealed that H_2O_2 release is significantly increased in brain slices from chemotherapy treated rats. Hence, the mechanism of PCCI can be a consequence of neuronal degeneration induced by enhanced free radical activity. Behavioral studies done by our collaborator (Dr. David. P. Jarmolowicz), further confirmed our results. In addition, neuro-protecting agent (KU-32) suppressed the elevated H_2O_2 levels. However, more investigations are required including studies on demyelination to assess the role of H_2O_2 on the onset of post chemotherapy cognitive impairment. Chemotherapy drugs can inhibit neuronal signaling by affecting myelination.[2] Therefore it is important to investigate how chemotherapy can affect myelination. Also it is important to utilize more complex and rigorous behavioral paradigms in future studies. Furthermore, Fluorescence imaging of H_2O_2 in the MSN can be used to investigate its role in PCCI. There are several fluorescent dyes including Redoxfluor-1 (RF1) which can be used. Images can be acquired using a cascade CCD camera.[3] Using this method intracellular H_2O_2 levels can be directly visualized.

Moreover, a variety of chemotherapeutic agents including blood brain barrier permeable and impermeable, are currently been used in clinic are causing chemo brain. It is important to investigate the extent of free radical activity for each type of chemotherapeutic agent to have a better understanding.

In the future it would be interesting to probe H_2O_2 levels in Zebrafish whole brain which provide the advantage of high throughput screening.

References

1. Sanford, A. L.; Morton, S. W.; Whitehouse, K. L.; Oara, H. M.; Lugo-Morales, L. Z.; Roberts, J. G.; Sombers, L. A., Voltammetric detection of hydrogen peroxide at carbon fiber microelectrodes. *Anal. Chem.* **2010,** *82* (12), 5205-5210.

2. Dietrich, J.; Han, R.; Yang, Y.; Mayer-Proschel, M.; Noble, M., Cns progenitor cells and oligodendrocytes are targets of chemotherapeutic agents in vitro and in vivo. *J. Biol.* **2006,** *5* (7), 22.

3. Bao, L.; Avshalumov, M. V.; Patel, J. C.; Lee, C. R.; Miller, E. W.; Chang, C. J.; Rice, M. E., Mitochondria are the source of hydrogen peroxide for dynamic brain-cell signaling. *The Journal of neuroscience : the official journal of the Society for Neuroscience* **2009,** *29* (28), 9002-9010.